Natural Product Reports

ROYAL SOCIETY OF CHEMISTRY

REVIEW

View Article Online
View Journal | View Issue

Cite this: *Nat. Prod. Rep.*, 2025, **42**, 1344

Recent insights into the biosynthesis and biological activities of the peptide-derived redox cofactor mycofactocin†

Mark Ellerhorst, [a] Vadim Nikitushkin, [a] Walid K. Al-Jammal,[b] Lucas Gregor, [b] Ivan Vilotijević [b] and Gerald Lackner [*a]

Received 25th February 2025

DOI: 10.1039/d5np00012b

rsc.li/npr

Covering: 2011 to 2025

The importance of redox cofactors like nicotinamide adenine dinucleotide or flavin adenine dinucleotide as cofactors for enzymatic reactions in living organisms is widely known. However, many microbial species also employ unusual redox cofactors such as the coenzyme F_{420} or the peptide-derived pyrroloquinoline quinone (PQQ). In this review, we introduce the reader to the recently discovered bacterial redox cofactor mycofactocin (MFT), a valine-tyrosine-derived small molecule of the class of ribosomally synthesized and post-translationally modified peptides (RiPPs) with remarkable biosynthetic and functional similarities to PQQ. The cofactor plays an important role in the reoxidation of non-exchangeable nicotinamide redox cofactors of specialized oxidoreductases in mycobacteria and related actinobacteria. We highlight the bioinformatic discovery of the mycofactocin gene cluster and its auxiliary genes, present strategies for the chemical synthesis of the cofactor, and take a detailed look at the biosynthesis of the glycosylated molecule. Subsequently, the diverse mycofactocin-inducing

[a]*Chair of Biochemistry of Microorganisms, University of Bayreuth, Germany. E-mail: gerald.lackner@uni-bayreuth.de*

[b]*Institute for Organic Chemistry and Macromolecular Chemistry, Friedrich Schiller University Jena, Germany*

† Electronic supplementary information (ESI) available. See DOI: https://doi.org/10.1039/d5np00012b

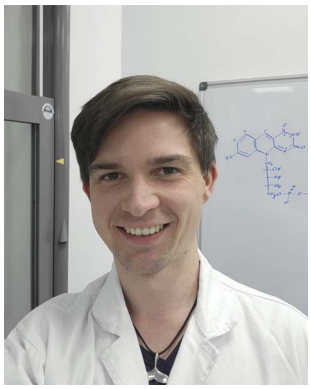

Mark Ellerhorst

Mark Ellerhorst obtained his BSc and MSc degrees from the Friedrich-Schiller University of Jena in 2018 and 2020, respectively, and worked during his master's thesis on the role of mycofactocin in the antibiotic-producing bacterium Saccharopolyspora erythraea in the group of Gerald Lackner at the Leibniz Institute for Natural Product Research and Infection Biology. Subsequently, he began his PhD work in the same group, focusing on the elucidation of mycofactocin methylation and its physiological role in Mycolicibacterium smegmatis and other Actinobacteria. In 2024 he moved to the University of Bayreuth, Campus Kulmbach, where he continues his PhD project.

Vadim Nikitushkin

Vadim Nikitushkin obtained his PhD in the Russian Academy of Sciences (A. N. Bach Institute of Biochemisty). During doctoral studies he investigated molecular mechanisms of reactivation of dormant mycobacteria under the influence of mycobacterial peptidoglycan cleavage products (muropeptides). Applying bioanalytical methods, he revealed the structures of porphyrin molecules accumulated by dormant forms of mycobacteria. In 2022, he joined Prof. Dr Gerald Lackner's group at the Leibniz Institute for Natural Product Research and Infection Biology in Jena, where he worked on mycobacteria under different physiological conditions and stress factors. Current interests comprise application of omics-based approaches for the investigation of cofactor metabolism.

conditions and associated oxidoreductase families are reviewed, and a potential electron transfer route from high-energy alcohols *via* mycofactocin to oxygen as a final electron acceptor is presented. The review concludes with a comparison of the physiological roles of PQQ and MFT, and an outlook for future research questions and potential biotechnological applications of mycofactocin.

Walid K. Al-Jammal

Walid Al-Jammal earned his BSc and MSc in Chemistry from Jordan University of Science and Technology, Jordan where he focused on the regioselective synthesis of iodinated aromatics via Suzuki–Miyaura cross-coupling. In 2019, he began his PhD with Prof. Dr Ivan Vilotijević at Friedrich Schiller University Jena, working on the total synthesis of mycofactocins and paleofuran A, metal-carbenoid reactions for the synthesis of C–P, C–B, and C–Si compounds, and the development of asymmetric phosphine catalysis. As a postdoctoral researcher in the group of Prof. Dr Ivan Vilotijević, he is currently developing modified lipopeptide mediators to study polymicrobial interaction.

Ivan Vilotijević

Ivan Vilotijević studied chemistry at University of Belgrade, Ohio State University and University of Illinois Urbana-Champaign. He earned a PhD in organic chemistry from Massachusetts Institute of Technology working on epoxide-opening cascade reactions aimed at synthesis of ladder polyether natural products. After a postdoctoral appointment at Max Planck Institute of Colloids and Interfaces working on synthesis of glycosylphosphatidylinositols and GPI-anchored proteins, he joined Friedrich Schiller University Jena where he currently serves as a professor for organic synthesis methods. His team develops novel catalytic methods for synthesis of complex organic molecules and pursues target-oriented synthesis of bioactive molecules and biological probes.

Lucas Gregor

Lucas Gregor earned his BSc and MSc degrees in chemistry from the Friedrich Schiller University Jena in 2021 and 2023, respectively. He completed his bachelor's thesis in the group of Prof. Dr Arndt and his master's thesis on the total synthesis of mycofactocins in the group of Prof. Dr Vilotijević. Currently pursuing his PhD in the same group, he continues working on the synthesis of mycofactocins and explores novel strategies for regioselective radical functionalizations through hydrogen atom transfer (HAT).

Gerald Lackner

Gerald Lackner studied biochemistry at Friedrich Schiller University in Jena, Germany. He earned his PhD in 2011 at the Leibniz Institute for Natural Product Research and Infection Biology (Leibniz-HKI). As a Feodor Lynen fellow at ETH Zurich, his research centered on unculturable bacteria producing bioactive compounds. In 2016, he became junior group leader at the Leibniz-HKI focusing on the biosynthesis of the cofactor mycofactocin and its biological activities. In 2023, he was appointed as a full professor for Biochemistry of Microorganisms at the University of Bayreuth based at the Campus Kulmbach, where he continues his work on bioactive natural products.

1. Peptide-derived redox cofactors

Life, as we know it, is impossible without enzymes that catalyse specific metabolic reactions. An important class of enzymes are oxidoreductases which facilitate a broad range of redox reactions both in dissimilatory as well as in assimilatory metabolic pathways. The limited chemical variety of amino acids in oxidoreductases necessitates the employment of redox-active cofactors to perform redox catalysis and electron transport. Typical redox cofactors are metals (especially iron, manganese, nickel and copper),[1] iron-sulphur clusters,[2] or small organic molecules like flavins or quinones.[3,4] Organic cofactors exhibit a remarkable structural diversity,[4] and the metabolic pathways leading to their formation are equally varied. Yet, a notable subset of cofactors shares a common biosynthetic origin, as they are derived from peptides. The most studied example of a peptide-derived redox cofactor is pyrroloquinoline quinone (PQQ), which was initially associated with the activity of glucose dehydrogenases[5] and methanol dehydrogenases.[6–8] PQQ is a quinone cofactor that non-covalently binds to the active site of a corresponding dehydrogenase. These enzymes, usually referred to as quinoproteins, are present in the periplasmic space of predominantly Gram-negative bacteria and perform oxidations of an alcohol substrate to its corresponding carbonyl product with the concomitant formation of the reduced $PQQH_2$ cofactor (Fig. 1).[10–14]

1.1 The biosynthesis of PQQ

The elucidation of the biosynthesis of PQQ demonstrated that it follows the logic of ribosomally synthesized and post-translationally modified peptides (RiPPs, Fig. 2).[15] The biosynthesis of a RiPP starts with the translation of a short precursor peptide (Fig. 2), typically consisting of a leader and a core region and, in some cases, a follower peptide located at the C-terminus. Maturation enzymes install post-translational modifications at the core region. Afterwards, a dedicated peptidase typically excises the modified core peptide from the precursor peptide backbone, resulting in the liberation of the modified core, *i.e.* the final RiPP natural product, leaving the leader and follower peptides as byproducts. In case of PQQ, the biosynthesis is accomplished by the gene products of the PQQ biosynthesis genes *pqqA-F/G*, which can be encoded as a biosynthetic gene cluster (BGC) (Fig. 3A).[11,16] PqqA is the precursor peptide, which harbours a core region located between the leader and a short follower peptide, framed by Glu and Tyr residues (Fig. 3B). A crucial step in the PQQ biosynthesis is the crosslinking of the C_9–C_{9a} atoms of the Glu and Tyr residues within the PqqA core region (Fig. 3C).[11,16] This

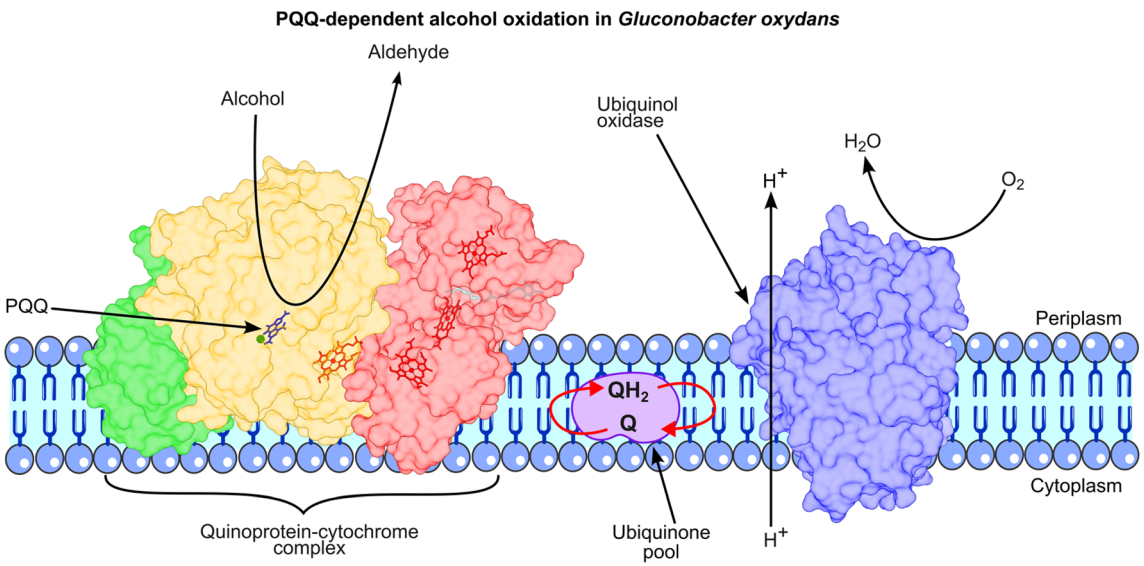

Fig. 1 Schematic visualisation of PQQ-dependent alcohol oxidation. As an example, a dehydrogenase complex from *Gluconobacter oxydans* is shown (PDB: 8GY2), consisting of three subunits: a small cofactorless subunit (green), participating in membrane binding, a large subunit (yellow), containing the PQQ cofactor (blue) and a heme *c* (red) binding site, where alcohol oxidation occurs. The third subunit (red) is the cytochrome *c* subunit, binding three heme *c* molecules, participating in electron transfer to the ubiquinone (Q/QH_2) pool (purple). The reduced quinone pool is regenerated by the ubiquinol oxidase[9] (AlphaFold 2 structure of UniProt: Q5FSK4). Source of "membrane-2d-bluelight" graphic: Servier (https://smart.servier.com/) licensed under CC-BY 3.0 Unported (https://creativecommons.org/licenses/by/3.0/).

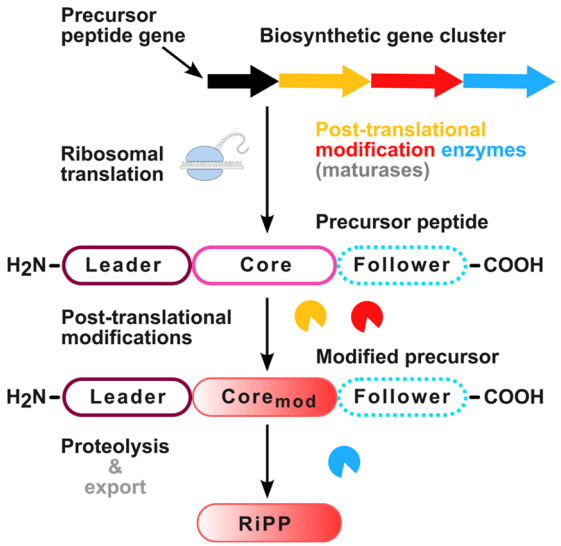

Fig. 2 General biosynthetic scheme of ribosomally synthesized and post-translationally modified peptides (RiPPs). The precursor peptide gene, *e.g. pqqA*, is transcribed and ribosomally translated. It usually contains an N-terminal leader sequence, a core region, and in some cases a follower peptide at the C-terminus of the core region. Maturases, *e.g.* PqqB-G, often encoded clustered with the precursor gene in a biosynthetic gene cluster, post-translationally modify the precursor peptide in its core region. Proteases then release the modified core from the peptide, which forms the final RiPP. Source of ribosome graphic: NIAID Visual & Medical Arts. (07/10/2024, https://bioart.niaid.nih.gov/bioart/448).

challenging reaction is performed by the radical *S*-adenosyl-L-methionine (rSAM) enzyme PqqE.[16,18] These enzymes coordinate [4Fe–4S]/[2Fe–2S] clusters and are capable of cleaving SAM to methionine and a 5′-deoxyadenosine radical.[18,19] However, for the successful cross-linking of the Glu and Tyr residues another protein is required, namely PqqD – a chaperone or RiPP recognition element (RRE), which was shown to form a trimeric complex with PqqA and PqqE (Fig. 3C).[16,20–23] To generate a free PQQ precursor molecule, the cross-linked Tyr–Glu core needs to be excised from the modified PqqA precursor peptide. This excision reaction is performed by the PqqF/G heterodimer if it is encoded in a particular genome.[24] Alternatively, the excision is achieved by non-specific cell-associated proteases.[24] The liberated diamino acid precursor is further oxidized by a specific iron-dependent hydroxylase PqqB[25] and spontaneously undergoes sequential condensation to the bicyclic intermediate AHQQ (3a-(2-amino-2-carboxyethyl)-4,5-dioxo-4,5,6,7,8,9-hexahydroquinoline-7,9-dicarboxylic acid).[16,25] The final oxidative steps are catalysed by PqqC – a cofactorless oxidase that performs an oxidation of AHQQ to PQQ, consuming three oxygen equivalents.[25,26] The resulting PQQ molecule (Fig. 3C) serves as a redox cofactor in PQQ-dependent dehydrogenase reactions as shown in Fig. 1.

1.2 Enzyme backbone-derived quinone cofactors

Besides PQQ, a couple of further peptide-derived quinone cofactors have been discovered, namely trihydroxyphenylalanine quinone (TPQ),[27] tryptophan tryptophylquinone (TTQ),[28] lysyl tyrosine quinone (LTQ),[29] and cysteine tryptophyl quinone (CTQ).[30] A commonality among this family of quinone cofactors is the extensive modification of tryptophan and tyrosine aromatic rings of the protein backbone resulting in corresponding quinones, followed by the formation of new C–N, C–S or C–C bonds (in case of TTQ, LTQ and CTQ).[11] It should be noted that these cofactors in contrast to PQQ are formed *in situ* on the polypeptide chain of the apoenzyme, and therefore can be attributed to the group of protein-derived cofactors, whereas PQQ originates from its own precursor peptide, not from its cognate dehydrogenase.

A more recently discovered peptide-derived redox cofactor, mycofactocin (MFT), is the focus of this review. Mycofactocin can be regarded as an analog to PQQ, sharing a striking number of similarities. Although their biosynthetic gene clusters are not directly related, both PQQ and mycofactocin are products of RiPP pathways. Their biosyntheses involve rSAM-catalysed cyclization reactions as a first step and ultimately produce redox-active cofactors. In the following sections, we will recapitulate the discovery of the cofactor and explore recent advances concerning the structure elucidation, biosynthesis, and physiological roles of mycofactocin. We will finish with an outlook into the possible medical and biotechnological applications of the mycofactocin system.

2. Discovery of mycofactocin

The mycofactocin biosynthesis genes came into focus as a result of a comparative genomics study, aimed at the identification of potential novel cofactors.[31] To this end, an approach developed during a previous genomic profiling study that linked coenzyme F_{420} biosynthesis genes to genes encoding F_{420}-dependent enzymes was exploited as a strategy to discover unknown cofactors.[32] In particular, it was speculated that cofactor biosynthesis might involve radical *S*-adenosyl methionine (rSAM) domain-containing enzymes as known from PqqE (PQQ biosynthesis) or FbiC (coenzyme F_{420} biosynthesis). Furthermore, it was assumed that the presence of this rSAM gene should be tightly linked, *i.e.* co-occur genome-wide, with further biosynthetic genes and that the occurrence of these biosynthesis genes should correlate with gene families encoding putative cofactor-dependent enzymes. Using this Partial Phylogenetic Profiling strategy, the study revealed a gene encoding an rSAM enzyme belonging to the IPR023913 family (MftC, Table 1).[31] The gene strictly clustered locally with several other putative biosynthetic genes, one of which appeared to be a short open reading frame encoding for a putative precursor peptide with a conserved Val–Tyr carboxy terminus (MftA, IPR023988). As expected for a redox cofactor, its BGC was found to have a significant tendency to co-occur with oxidoreductases, in this case with members of three oxidoreductase families (IPR023985, IPR023921, IPR001670; Table 1). The finding that the presence of these oxidoreductases strictly depends on the presence of biosynthetic genes strongly supported the idea that they might require the product of the putative BGC as a cofactor. The identified BGC mainly occurred in mycobacteria,

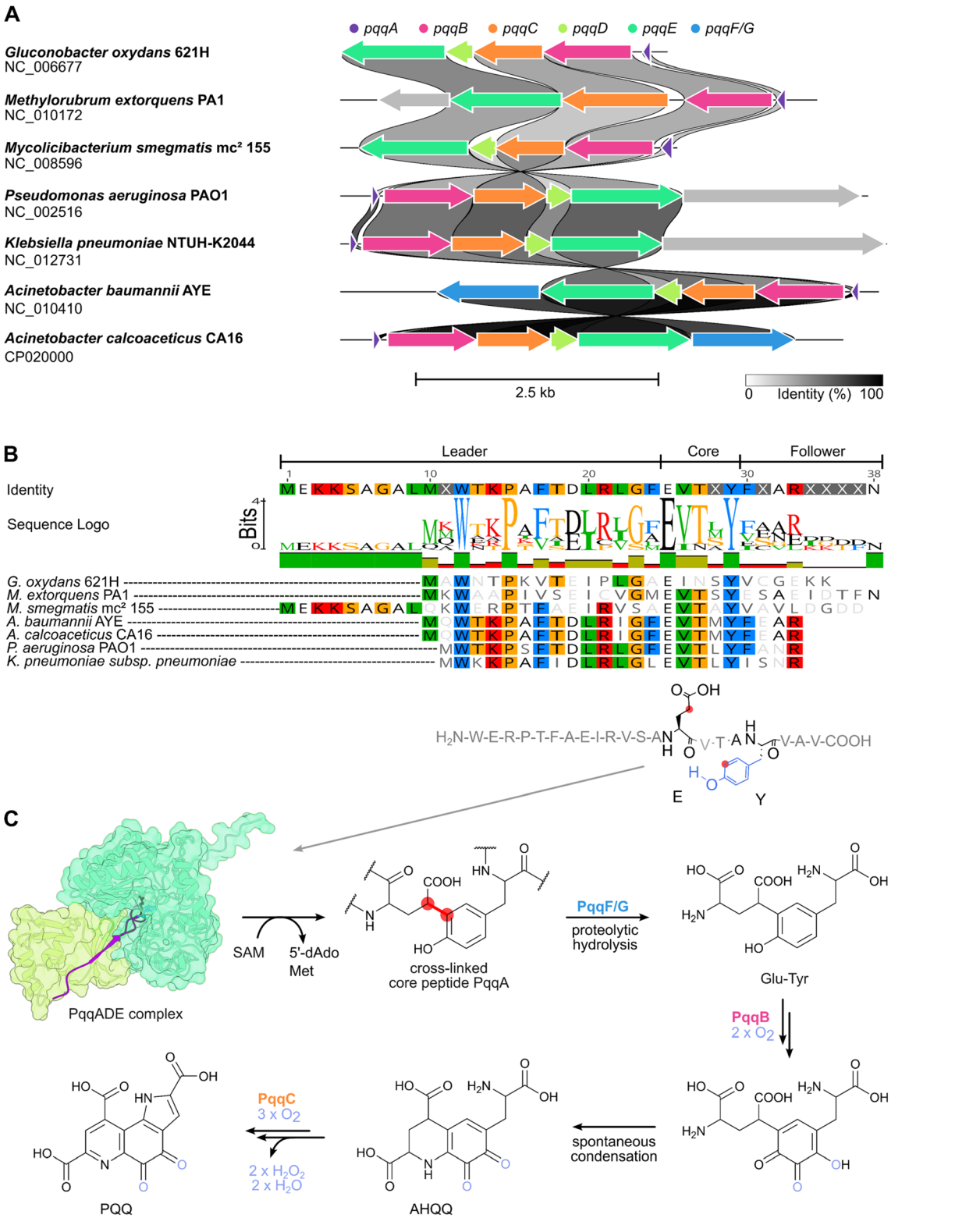

Fig. 3 The PQQ biosynthetic gene cluster and PQQ biosynthesis. (A) Biosynthetic gene clusters of PQQ in different organisms. (B) Sequence alignment of the PqqA peptide shows conserved glutamate (E) and tyrosine (Y) residues essential for PQQ core formation. Alignment generated in Geneious Prime 2024.0.7 (https://www.geneious.com). (C) PQQ biosynthesis. PqqA, the PQQ precursor peptide, is bound by the PqqDE complex consisting of the chaperone PqqD and the radical SAM enzyme PqqE. The PqqF/G heterodimer promotes liberation of the core peptide but seems to be non-essential for the PQQ biosynthesis in some organisms. The metallolactamase PqqB and the oxidase PqqC perform sequential oxidation and cyclisation.[16] Visualisation of the PqqADE complex was achieved with AlphaFold 2. The model with the highest parameter values for pLDDT, pTM and iPTM was selected.[17] Wavy lines indicate peptide bond connections to the PqqA backbone peptide. SAM – *S*-adenosyl-L-methionine, 5′-dAdo – 5′-deoxyadenosine, Met – methionine.

Table 1 Protein families associated with the mycofactocin system. In 2018, the TIGRFAM database[33] was integrated in the NCBIfam database.[34] Subsequently, protein families from different databases, such as TIGRFAM and PFAM, were integrated to InterPro entries starting in 2022.[35] Thereby, common identifiers for protein families used in studies relevant to mycofactocin research might be superseded. A mapping of identifiers in different databases is provided for relevant MFT-associated protein families below. Studied members of each family are listed with their UniProt identifiers and a protein data bank (PDB) crystal structure identifier if available. Members of the mycofactocin-specific IPR026338 family can often also be described by the hidden Markov model of the IPR001670 alcohol dehydrogenase superfamily. CHP – conserved hypothetical protein, OYE – old yellow enzyme, NDMA – 4-nitroso-*N*,*N*-dimethylaniline

Description	*In vitro* studied examples	TIGRFAM/PFAM/NCBIFam	InterPro database entry
MftA – mycofactocin precursor peptide	P0DUE9 (*Mycobacterium ulcerans* Agy99)[36]	TIGR03969	IPR023988
MftB – mycofactocin chaperone	A0PM48 (*M. ulcerans* Agy99)[36]	TIGR03967	IPR023850
MftC – mycofactocin rSAM maturase	A0PM49 (*M. ulcerans* Agy99)[36]	TIGR03962	IPR023913
MftD – pre-mycofactocin synthase	A0PM50 (*M. ulcerans* Agy99)[37]	TIGR03966	IPR023989
MftE – mycofactocin precursor peptide peptidase	A0PM51 (*M. ulcerans* Agy99)[38]	TIGR03964	IPR023871
MftF – mycofactocin glycosyltransferase	—	TIGR03965	IPR023981
MftM – mycofactocin oligosaccharide methyltransferase	—	NF041255	—
MftR – mycofactocin transcriptional regulator	A0QSB5 (*M. smegmatis* mc^2 155)[39] P9WMB7 (*M. tuberculosis* H37Rv)[40]	TIGR03968	IPR023851
MftG – glucose-methanol-choline oxidoreductase, bacteria	A0QSC2 (*M. smegmatis* mc^2 155)[41]	TIGR03970 NF038210 (restricted to genus *Dietzia*) TIGR04542 (restricted to genus *Gordonia*)	IPR023978
Mycofactocin-dependent oxidoreductase/ SDR_subfam_1	A0QSA5 (*M. smegmatis* mc^2 155)[37] B1MLR7 (PDB: 3S55, *Mycobacteroides abcessus* ATCC 19977)[42] A0A0H2ZWY3 (PDB: 3TC7, *Mycobacterium avium* 104)[42] A0A0H2ZTN5 (PDB: 3UVE, *M. avium* 104)[42] A0A0H2ZU39 (PDB: 4RGB, *M. avium* 104)[42] A0A0M3KKT7 (PDB: 3PXX, *M. avium* 104)[42] A0A0H2ZYS9 (PDB: 5EJ2, *M. avium* 104)[42] Q73SC8 (PDB: 3PGX, *Mycolicibacterium paratuberculosis* K-10)[42] Q73W00 (PDB: 3SX2, *M. paratuberculosis* K-10)[42] Q73X99 (PDB: 3TSC, *M. paratuberculosis* K-10)[42] Q9RA05 (*Rhodococcus erythropolis* DCL14)[43] Q53062 (*R. erythropolis* NI86/21)[44]	TIGR03971	IPR023985
Alcohol dehydrogenase, zinc-type, ADH_Zn_actinomycetes	P80175 (*Amycolatopsis methanolica* 239)[45,46] P81747[a] (*Rhodococcus opacus* DSM 1069)[47]	TIGR03989	IPR023921
NDMA-dependent methanol dehydrogenase, NDMA_methanol_DH	Q9RCG0 (*A. methanolica* 239)[48,49] C5MRT8 (*Mycobacterium* sp. JC1)[50] A0R5M3 (*M. smegmatis* mc^2 155)[51] Q53062 (*R. erythropolis* NI86/21)[44] A5LHA1 (*R. erythropolis* N9T-4)[52]	TIGR04266	IPR026338
Alcohol dehydrogenase, iron-type, ADH_Fe	Q9RCG0 (*A. methanolica* 239)[48,49] C5MRT8 (*Mycobacterium* sp. JC1)[50] A0R5M3 (*M. smegmatis* mc^2 155)[51] Q53062 (*R. erythropolis* NI86/21)[44] A5LHA1 (*R. erythropolis* N9T-4)[52]	PF00465	IPR001670
CHP03996, oxidoreductase/OYE_1	—	TIGR03996	IPR023967
CHP03977, oxidoreductase/OYE_2	—	TIGR03977	IPR023987
Mycofactocin-dependent oxidoreductase/ SDR_subfam_2	—	TIGR04504	IPR030981
Mycofactocin-dependent oxidoreductase/ SDR_subfam_3	—	NF040490	—
Mycofactocin-dependent oxidoreductase/ SDR_subfam_4	—	NF040491	—

[a] Full protein sequence not available. The list of *in vitro* studied examples contains only proteins studied in isolated form and is non-exhaustive due to lack of sequence data for some studied proteins.

including the causative agent of tuberculosis, *Mycobacterium tuberculosis*.[31] The predicted product of the BGC was named mycofactocin, a portmanteau of **myco**bacteria, PQQ co**fact**or and bacterio**cin**s, with which it presumably shared a common function and biosynthetic logic, respectively.[31]

3. Structure and chemical synthesis of mycofactocin

The term mycofactocin designates a group of closely related compounds consisting of a peptide-derived aglycone, *i.e.* a redox-active core, and an oligosaccharide. The structure of mycofactocin mMFT-8, shown in Fig. 4A, is illustrative of the general structure of mycofactocins where the redox core structure is non-variable while the attached oligosaccharide varies in length and modifications with numerous different glycoforms shown to exist *in vivo*.[53] A table of known and hypothetical mycofactocin structures including their SMILES, sum formulas, and theoretical monoisotopic mass is provided in the ESI (ESI, mycofactocin_SMILES.xlsx).†

The redox-active aglycone core structure, MFT-0, is a highly substituted α-keto-γ-butyrolactam carrying two geminal methyl substituents at the C4 position and a 4-hydroxybenzyl substituent at C5 (Fig. 4B). The reduced aglycone, MFT-0H_2, formerly also named premycofactocinol PMFTH_2, where H_2 indicates the reduced form, features an alcohol instead of the ketone in C3 position of the γ-butyrolactam. Structurally, these aglycones appear to be derivatives of a Tyr–Val dipeptide that has undergone decarboxylation and cyclization by bond formation between the C3 of valine and C2 of tyrosine which creates the C4–C5 bond of the resulting γ-butyrolactam core structure. The α-amino function apparently is further converted either by substitution to form the alcohol in MFT-0H_2 or by oxidation to form the ketone in MFT-0. This hypothesis is further corroborated by identification of the related aglycons AHDP-0 and GAHDP-0 that feature an α-amino or α-amido instead of α-keto or α-hydroxy substituent in the γ-butyrolactam core (Fig. 4B). Absolute stereochemical assignment of natural MFT-0 as well as the relative stereochemistry of MFT-0H_2, AHDP and GAHDP remain unknown.

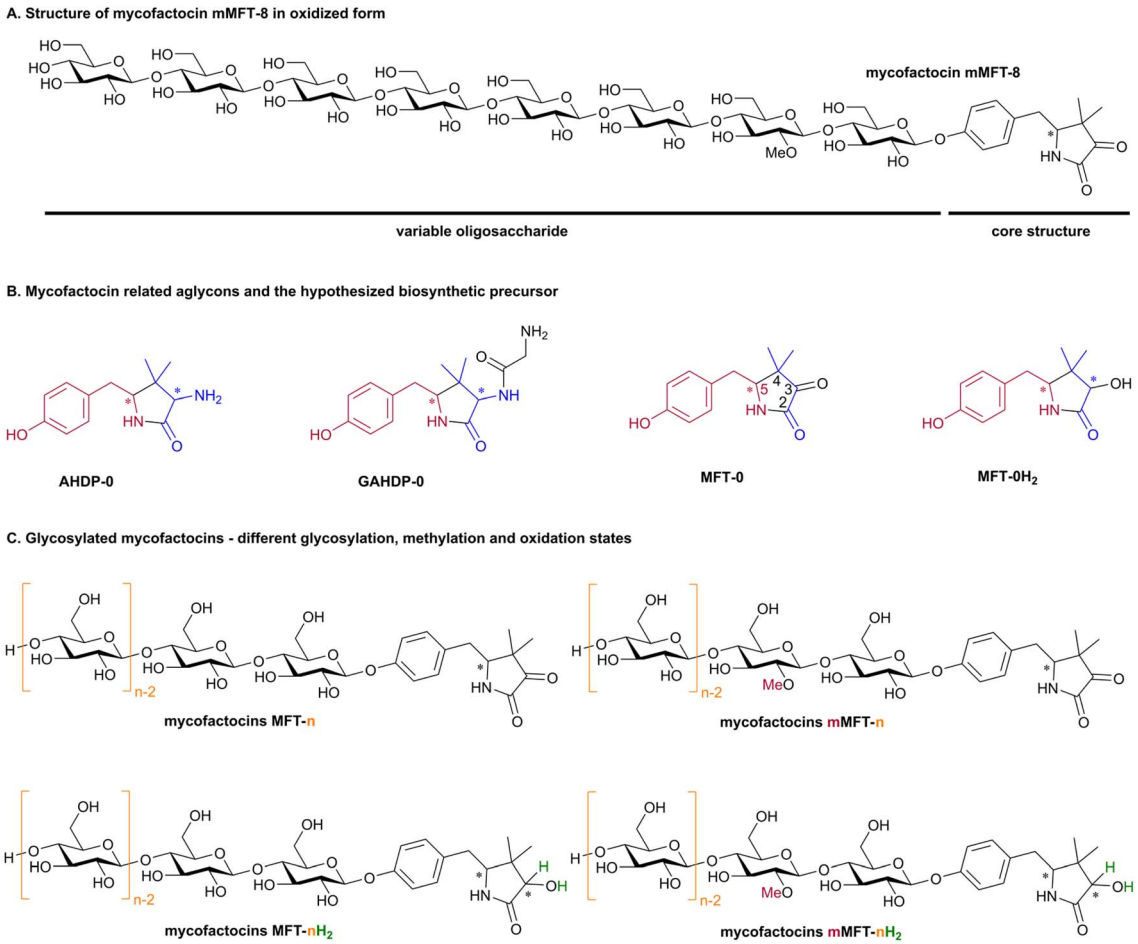

Fig. 4 Structural diversity and nomenclature of mycofactocins. (A) Structure of mycofactocin mMFT-8 in its oxidized form depicting the redox active core structure and the variable oligosaccharide. (B) Mycofactocin-related aglycones. (C) Structures of glycosylated mycofactocins from *M. smegmatis* extracts: (m)MFT-*n*(H_2): "m" indicates the presence of methyl ether on the second glucose unit; "*n*" indicates the number of glucose residues in β-1,4-glucan oligosaccharide with $n = 0$ to 9; "H_2" indicates the reduced form of the α-keto-γ-butyrolactam redox core. Stereochemical assignment for aglycones and hypothesized biosynthetic precursors is unknown, but theoretical stereogenic centres have been marked with asterisks for clarity.

The phenol oxygen in both MFT-0 and MFT-0H_2 can carry a β-1,4-glucan consisting of up to nine glycosyl residues resulting in mycofactocins MFT-*n* and MFT-*n*H_2 respectively, where "*n*" indicates the number of glucose residues in the oligosaccharide in a range from 1 to 9. Both the oxidized (MFT-*n*) and reduced (MFT-*n*H_2) glycosylated forms (Fig. 4C) have been identified in natural extracts.[53,54] Further derivatives that have been isolated and characterized carry an *O*-methyl ether in C2 position of the second glucose unit, counting from the core structure. The methylation results in mMFT-*n* and mMFT-*n*H_2, where "m" indicates the presence of this methyl ether (Fig. 4C).[53] The general term used for oxidized mycofactocins is mycofactocinones and that for reduced mycofactocins is mycofactocinols, following the nomenclature of quinones and quinols as used, for example, for PQQ.

Structural assignments of both aglycones and different glycoforms has been established based on extensive tandem MS and NMR studies of material isolated from *Mycolicibacterium smegmatis* mc^2 155. Confirmation of the identities of MFT-0 and MFT-0H_2 was provided by chemical synthesis by the teams of Latham and Michel,[55] and of Vilotijević and Lackner.[54] The reported retrosynthetic approach to MFT-0 and MFT-0H_2 (Scheme 1A) is based on late stage α-oxidation of the γ-butyrolactam **1** which was envisioned from the nitro ester **2** *via* reduction of the nitro group and cyclization *via* amid formation. The required precursor **2** could be prepared *via* Michael addition of the anion derived from the nitroalkane **4** to the acrylate **3**.

The synthesis of MFT-0 and MFT-0H_2 is described in Scheme 1B.[54] The suitable nitroalkane **5** is available in two steps *via* Henry reaction of the corresponding benzaldehyde and nitromethane followed by hydrogenation of the alkene. Nitroalkane **5** undergoes Michael addition to methyl 3,3-dimethylacrylate **3** promoted by tetrabutylammonium fluoride. Subsequent reduction of the nitro group in **6** to amine triggers a cyclization resulting in the γ-butyrolactam **7a** and the corresponding enamide **7b** which is easily reduced to **7a** by hydrogenation in the presence of palladium on carbon. Boc protection followed by Davis' oxidation completes the α-hydroxy-γ-butyrolactam core of the protected MFT-0H_2 **8**. MFT-0H_2 was obtained through removal of Boc and methyl protecting groups by treatment with boron tribromide. Oxidation of alcohol **8** to the corresponding ketone followed by deprotection yields MFT-0. Comparison of the synthetic material to material isolated from natural sources confirmed the identities of MFT-0H_2 and MFT-0. It should be mentioned, however, that the core molecules MFT-0 and MFT-0H_2 as well as ADHP-0 have not yet been observed in bacterial extracts, but only appear after cellulase treatment of glycosylated mycofactocins, thereby liberating the core structures (Fig. 4B). Previous evidence for the existence of the core aglycone structures in bacterial extracts appears to be a mass spectrometry in-source fragment artifact of glycosylated mycofactocin.[53,54] Future research will have to focus on the investigation of the relative and absolute configuration of mycofactocin and their potential effects on biologically-relevant catalytic activities.

4. Biosynthesis of mycofactocin

4.1 The biosynthetic pathway of mycofactocin

Experimental and bioinformatic efforts revealed that the mycofactocin BGC comprises the genes *mftABCDEF* and in approximately thirty percent of MFT BGC-encoding bacteria also the gene *mftM* (Fig. 5A).[54] The MFT BGC can be found primarily in mycobacteria but also other actinobacteria and even archaea. For a detailed description of the phylogenetic distribution of this gene cluster, we refer the reader to the first review published on mycofactocin by Ayikpoe *et al.*[57] Fig. 7 depicts the current hypothesis of mycofactocin biosynthesis

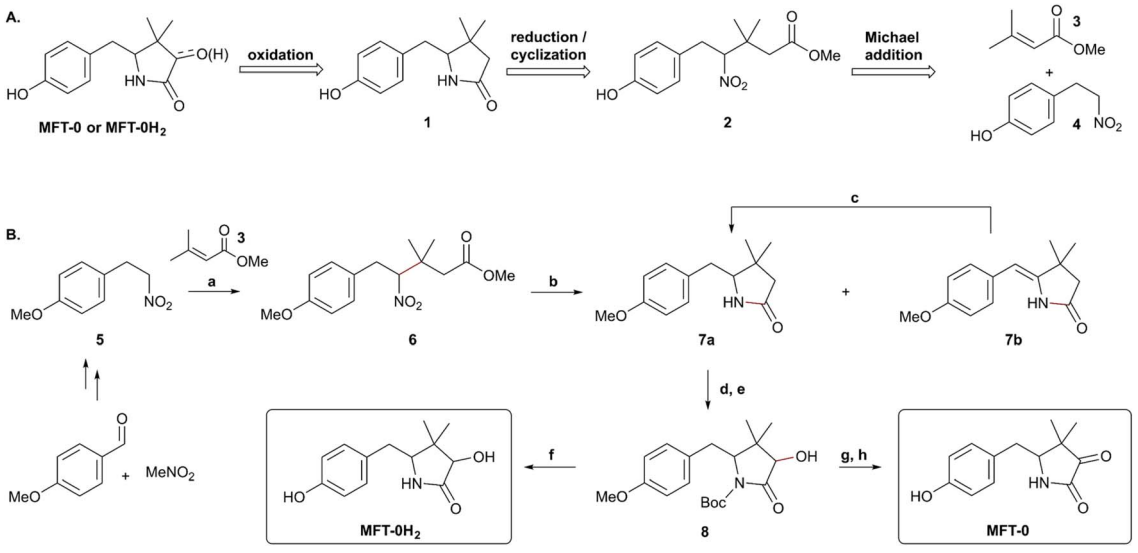

Scheme 1 A) Retrosynthetic analysis of mycofactocins MFT-0 and MFT-0H_2 (protecting groups are omitted). (B) Synthesis of mycofactocins MFT-0H_2 and MFT-0. (a) Methyl-3,3-dimethyl acrylate **3**, TBAF, THF, 40 °C, 80 h, 47%; (b) H_2, Raney-Ni, MeOH, 60 °C, 12 h, 7a: 51%, 7b: 34%; (c) H_2, Pd/C, MeOH, rt, 12 h, 96%; (d) Boc_2O, Et_3N, DMAP, CH_2Cl_2, rt, 12 h, 73%; (e) Davis reagent, LDA, THF, −78 °C to rt, 4 h, 38%; (f) BBr_3, CH_2Cl_2, 0 °C, 2 h, 30%; (g) $(COCl)_2$, DMSO, Et_3N, CH_2Cl_2, −78 °C, 2 h, 72%; (h) BBr_3, CH_2Cl_2, 0 °C, 2 h, 21%.

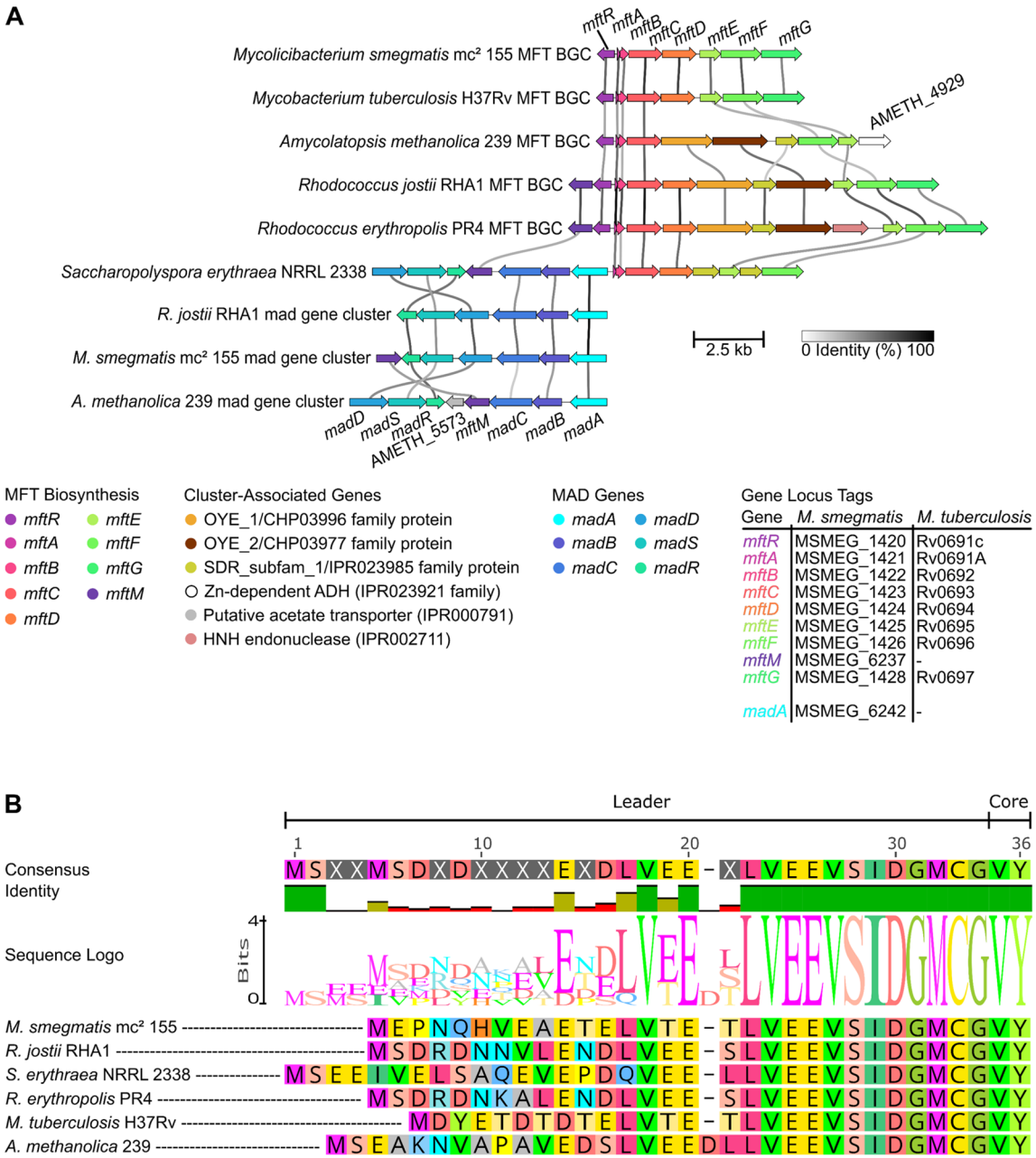

Fig. 5 The genetic landscape of mycofactocin and the conservation of MftA. (A) The mycofactocin-dependent alcohol degradation (*mad*) gene cluster can be but is not necessarily encoded adjacent to the mycofactocin BGC. Species encoding a gene cluster for methylated mycofactocin, *i.e.* encoding an *mftM* homolog aside the regular *mftABCDEF* gene cluster, also encode *madA*.[54] Cluster-associated genes are not present in every MFT or MAD locus. Line darkness indicates gene nucleic acid sequence similarity. Arrow length represents gene length. Colours highlight homologous genes. Plot created with clinker.[56] (B) Shown is a multiple sequence alignment of different MftA highlighting the strong conservation of the C-terminal VY-core, the precursor structure of mycofactocin. Alignment generated in Geneious Prime 2024.0.7 (https://www.geneious.com).

catalysed by the gene products of the MFT BGC *mftABCDEF*(*M*). The order of the biosynthetic steps, however, is ambiguous with currently available data. Thus, multiple scenarios will be discussed in this chapter along with the individual functions of the MFT BGC genes, starting with the hypothetical pathway that would result in the redox active core structure MFT-0.

In vitro studies showed that MftA is first bound by MftB, its chaperone or RRE. Afterwards, it is modified by the [4Fe–4S]-binding enzyme MftC, the rSAM enzyme that led to the discovery of the mycofactocin BGC. MftC catalyses a two-step oxidative decarboxylation and cyclization of the highly conserved C-terminal VY core peptide of MftA (Fig. 5B) which results in the formation of MftA*, containing a valine–tyrosine crosslink (Fig. 6).[36] The modified core is cleaved off of MftA* by the mycofactocin peptidase MftE between the C-terminal glycyl and (modified) valyl residues,[58] forming AHDP, *i.e.* AHDP-

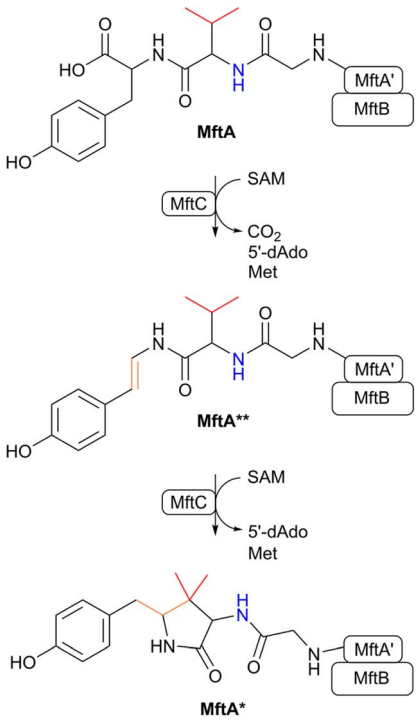

Fig. 6 The two-step MftC-mediated decarboxylation and cyclization of MftA. The mycofactocin precursor peptide MftA is bound by its chaperone (RRE) MftB and modified in a radical *S*-adenosyl methionine-dependent two-step reaction by MftC to the cyclized mycofactocin precursor MftA*. During the reaction, the apparently unstable intermediate MftA** is formed.[36] SAM – *S*-adenosyl-L-methionine, 5′-dAdo – 5′-deoxyadenosine, Met – methionine.

0 since no glucose moieties are attached (Fig. 7).[38] AHDP, which carries a free amine originating from valine, can subsequently undergo oxidative deamination by the flavin mononucleotide (FMN)-dependent deaminase MftD to produce the redox active MFT core structure with a redox potential (midpoint potential) of −255 mV *vs.* a standard hydrogen electrode (SHE) determined for MFT-0 *via* cyclic voltammetry.[37] This AHDP-0-derived redox pair is called MFT-0 (oxidized form)/MFT-0H_2 (reduced form, Fig. 4C).

Investigation of bacterial mycofactocin additionally revealed that the core structure was glycosylated with up to nine glucose moieties with β-1,4-linkage attached to the hydroxyl group of the former tyrosyl residue forming MFT-*n* (Fig. 4C and 7).[53] This glycosylation was shown to be mediated by MftF, a member of the glycosyl transferase family IPR023981, whose gene is an integral part of the mycofactocin gene locus.[31] Enzymatic redox studies with natural mycofactocin from *Mycolicibacterium smegmatis* mc^2 155, the model organism for mycofactocin research, provided support for the existence of redox active MFT-*n* with a two-electron hydride transfer occurring on the core structure as shown by *in vitro* studies described above (Fig. 4C and 8).[53]

As described in chapter 3, the oligosaccharide can further be singly methylated on the second glucose unit resulting in methylmycofactocinone-*n* (mMFT-*n*) and methylmycofactocinol-*n* (mMFT-*n*H_2). The evidence for methylated mycofactocin derivatives implied the existence of a methyltransferase capable of catalysing this very specific 2-*O*-methylation reaction. In the mycofactocin BGC of *M. smegmatis*, however, no such putative methyltransferase was found (Fig. 5A), and neither was one predicted to be part of the MFT BGC by Daniel H. Haft's seminal bioinformatics study.[31] In 2022, the groups of Lackner and Vilotijević identified the gene responsible for this methylation in *M. smegmatis*, *mftM*, belonging to the novel mycofactocin-specific protein family NF041255.[54] The gene is not located in the vicinity of the mycofactocin BGC in the genome of this strain. However, it was found to be clustered with the putative mycofactocin-dependent alcohol dehydrogenases MSMEG_6239 (*madD*) and MSMEG_6242 (*madA*). In several *Rhodococcus* strains, the *mftM* gene was subsequently found to be encoded directly upstream of the mycofactocin BGC in reverse orientation (Fig. 5A). In species lacking an MSMEG_6242 homolog, *e.g. M. tuberculosis*, the *mftM* gene was missing, too. In accordance with this finding, no methylated mycofactocin species were found in these *madA*- and *mftM*-negative organisms.[54]

4.2 The order of the mycofactocin biosynthetic steps

While all genes of the mycofactocin BGC, *mftABCDEF*(*M*), were functionally described, the order of the biosynthetic steps *in vivo* is not yet fully elucidated. It is reasonable to assume that the MftE peptidase reaction should occur before the MftD reaction that converts the amino group of the modified valine of AHDP-*n*, which is only accessible after MftE-catalysed release of the modified RiPP core from MftA*-*n* (Fig. 7). However, it is unclear which mycofactocin congener or precursor is glycosylated, how the glucan chain length is regulated, and at which point the methylation takes place. It is possible that already the unmodified MftA precursor peptide is glycosylated since the hydroxyl group of the C-terminal tyrosyl residue does not appear to be directly involved in core maturation.[36,37] The glycosylation might also happen on the cyclized MftA* structure after the MftC reaction took place. However, neither of the two hypothesized peptides, *i.e.* MftA-*n* nor MftA*-*n*, were observed *in vivo* so far, independent of their glycosylation state. Metabolome data corroborated the hypothesis that the MftF reaction occurs before the MftD deamination reaction since glycosylated AHDP was found *in vivo* and a deletion of *mftF* resulted in complete absence of MFT-0(H_2),[53] *i.e.* upon loss of the MftF reaction, all potential downstream products of MftD were absent. The fact that intracellular AHDP-0 was strongly reduced as well might imply that MftF acts on a mycofactocin peptide precursor, before the MftE cleavage reaction took place. Possibly, the MftF protein might be structurally essential for the function of MftD and MftE *in vivo*, *e.g.* as an integral part of an enzyme complex. Alternatively, glycosylation could be essential for the stabilization or correct trafficking of biosynthetic intermediates *in vivo*. Recent work on the mycofactocin system of *Rhodococcus jostii* RHA1 supports the central role of MftF, since a Δ*mftF* mutant of this strain exhibited the same growth defect as a Δ*mftAB* strain of the same organism on ethylene glycol as the sole carbon source while both strains showed no growth defect on glucose,[59]

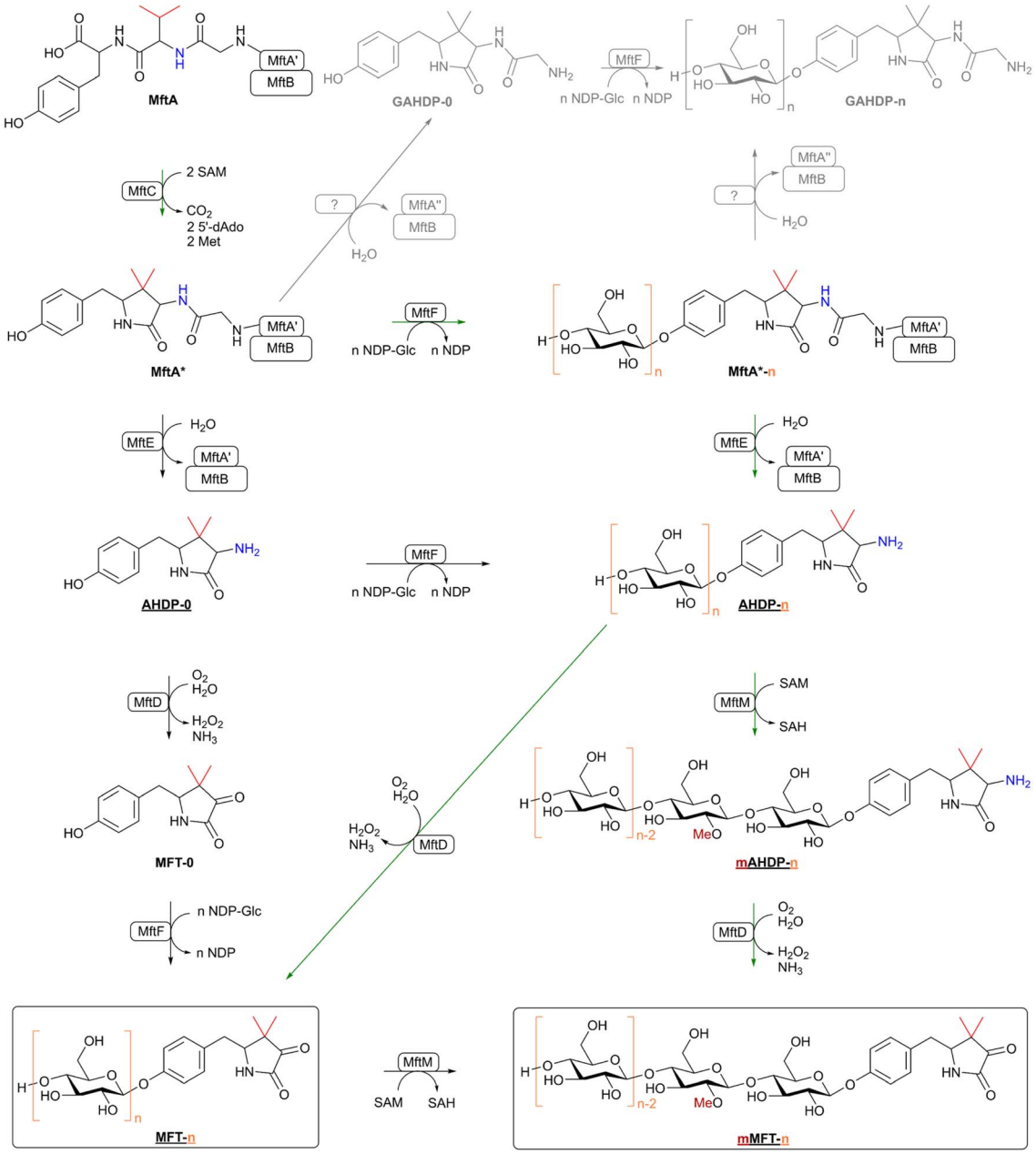

Fig. 7 Mycofactocin biosynthesis. Possible biosynthetic routes to mycofactocin (MFT-*n*) and methylmycofactocin (mMFT-*n*) are shown (final products in black boxes). Green arrows mark likely *in vivo* routes. The GAHDP pathway (light grey) represents a shunt pathway whose product carries an additional glycine as a result from an unspecific cleavage of the cyclized precursor MftA*. Molecules observed in natural extracts are underlined. MftA – mycofactocin precursor peptide, MftA* – MftA modified by MftC, MftA′ – MftA* N-terminus after MftE cleavage, MftA″ – MftA* N-terminus after unspecific cleavage resulting in the liberation of GAHDP-0/GAHDP-*n*, MftB – mycofactocin chaperone, MftC – mycofactocin radical SAM maturase, MftD – premycofactocin synthase, MftE – mycofactocin peptidase, MftF – mycofactocin glycosyltransferase, MftM – mycofactocin SAM-dependent methyltransferase, NDP-Glc – nucleotide diphosphate glucose, SAM – *S*-adenosyl methionine, SAH – *S*-adenosyl homocysteine, 5′-dAdo – 5′-deoxyadenosine, Met – methionine. Number of glucose moieties attached to the core through β-1,4-glycosydic bonds denoted by "*n*" with $1 \leq n \leq 9$. A complete list of hypothetical and observed mycofactocin congeners and precursors including their corresponding SMILES is provided in the ESI† "mycofactocin_SMILES.xlsx".

i.e. mycofactocin-mediated utilization of ethylene glycol as a carbon and energy source is lost in both cases which allows for the hypothesis that functional mycofactocin is not available in these strains. Finally, the methylation reaction mediated by MftM appears to occur before or independent of the MftD reaction, since methylated and glycosylated AHDP, *i.e.* mAHDP-*n*, was found *in vivo*.[53]

Thus, a likely biosynthetic route starts with the ribosomal translation of the MftA precursor, followed by cyclization by MftC, glycosylation by MftF and optional methylation by MftM. This modified glycosylated peptide is then cleaved between the

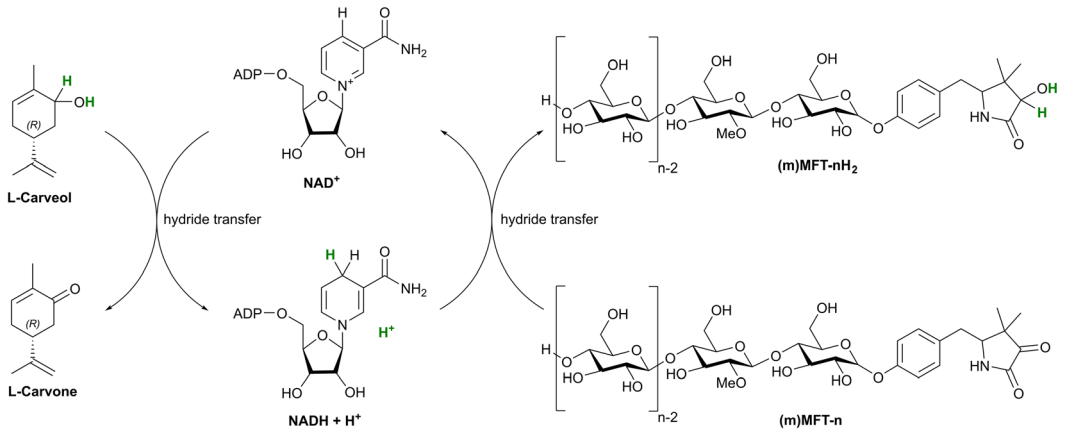

Fig. 8 Mycofactocin-mediated NAD(P) cofactor recycling. An example of the hypothetical mycofactocin-mediated internal NAD(P)$^+$ cofactor recycling is shown. A substrate, here L-carveol, is oxidized by an NAD$^+$-dependent dehydrogenase possessing an internal non-exchangeable NAD$^+$ as electron acceptor, *e.g.* LimC from *R. erythropolis* DCL14 (see Section 6.1). During the dehydrogenation reaction, two reducing equivalents are transferred onto NAD$^+$ leading to a reduction of the internal cofactor. To maintain enzyme functionality, the internal cofactor needs to be reoxidized from NADH to NAD$^+$. According to the mycofactocin hypothesis, this re-oxidation is achieved through a two-reducing-equivalents-transfer onto (methyl)mycofactocinone (m)MFT-*n* resulting in NAD(P)$^+$ and (methyl)mycofactocinol (m)MFT-*n*H_2. Reducing equivalents are highlighted in green. Both NAD$^+$ and NAD(P)$^+$ have been found as non-exchangeable cofactors of mycofactocin-dependent enzymes. ADP – adenosine diphosphate.

glycyl and modified valyl-tyrosyl residues of MtfA*-*n* and ends with the installation of the redox functionality by MftD by oxidative deamination of AHDP-*n* resulting in (m)MFT-*n* (Fig. 7).

4.3 The potential role of the side-chain modifications

A second open question concerns the functions of the glycosylation and methylation modifications. While it was shown that the methylation of the sugar chain confers resistance against cellulases *in vitro*,[54] it remains unclear which physiological roles these two unusual modifications play and how the glycosylation is regulated *in vivo*. The protective function might be directed towards host-derived cellulases, such as MSMEG_6752, a cellulase shown to degrade cellulose to cellobiose *in vitro*,[60] which might be co-expressed with the mycofactocin BGC. The role of the glucose methylation thus would be a protection against cofactor degradation by the host. This system, however, would only be functional in *mftM*-positive bacteria while the situation in bacteria that do not methylate mycofactocins needs to be further clarified. Further functions of mycofactocin methylation could be the modulation of cofactor solubility or the modulation of cofactor–enzyme interactions.

The glycosylation itself might aid in protein–cofactor interaction through hydrogen bonds between the glucose-derived hydroxyl groups and hydrophilic residues of mycofactocin-dependent enzymes. Similar functions are described for many cofactors' side chains, such as the nucleotide moiety of FAD.[61] Further examples are folates and coenzyme F_{420}, which carry an oligoglutamate side chain that strengthens their binding to enzymes.[62–64] Another function of the oligoglycosylation could be to prevent the leakage of the cofactor from the cell. The small and relatively apolar cyclic core molecules of many cofactors, such as the riboflavin core of FAD or the deazariboflavin core of coenzyme F_{420}, are often found to cross the cytoplasmic membrane.[65,66] This hypothesis is supported by the fact that mycofactocin-related aglycons, especially AHDP-0, can be detected in the supernatant of *M. smegmatis*.[54] A possible function of the glycosyl chain as a solubility-modulating part of mycofactocin awaits experimental investigation. Previous reports showed that increasing chain lengths of β-1,4-linked glucans are negatively correlated with water solubility, already for short-chain β-1,4-linked glucose oligosaccharides as present in mycofactocins.[67]

5. Physiological functions and regulation of mycofactocin

While the structure and biosynthesis of mycofactocin are fascinating from a chemical point of view, its physiological implications are equally intriguing. As outlined in the previous chapter, the mycofactocin system was found in part *via* co-occurrence of the BGC with oxidoreductases. Strikingly, one of the oxidoreductase families, encoding for short-chain dehydrogenases (SDR, *SDR_subfam_1* IPR023985), includes a carveol dehydrogenase from *Rhodococcus erythropolis* DCL14, which had been experimentally characterized long before mycofactocin was postulated (Table 1). It was shown to bind one non-exchangeable nicotinamide adenine dinucleotide (NAD) molecule per subunit in a tight non-covalent mode.[43] This usage of NAD as a tightly bound prosthetic group, which is reduced during oxidation of carveol to carvone, necessitates an external (diffusible) electron acceptor to reoxidize the internal nicotinamide cofactor. For *in vitro* experiments, an artificial electron acceptor, 2,6-dichlorophenol indophenol (DCPIP), was used to substitute the natural electron acceptor, which was unknown at the time of the study.[43] In the context of more recently published experiments discussed in chapter 6.1, it is highly likely

that the cryptic electron acceptor is mycofactocin. A hypothetical schematic representation of this mycofactocin-mediated NAD cofactor recycling reaction is presented in Fig. 8. This early finding already suggested a role of the cofactor in alcohol dehydrogenation reactions.

5.1 The role of mycofactocin in ethanol metabolism

Inspired by a previous study,[68] Krishnamoorthy *et al.*[69] attempted to study a potential role of mycofactocin in the utilization of cholesterol as a carbon source by different mycobacterial strains, such as *M. smegmatis* or *M. tuberculosis*, the causative agent of tuberculosis. Their investigations showed that it was not cholesterol that was used in a mycofactocin-dependent manner but it was instead the ethanol that was used to prepare cholesterol stock solutions, shifting the focus of mycofactocin-related metabolic processes towards ethanol utilization. Transcriptome profiling of *M. smegmatis* on medium containing ethanol *versus* glucose as the sole carbon source revealed upregulation of a gene encoding for the putative alcohol dehydrogenase MSMEG_6242 (*madA*, previously called *mdo* or *mno*). A knock-out mutant of this gene exhibited the same phenotype on ethanol as the mycofactocin knock-out mutants of *M. smegmatis*. However, it was able to grow on acetate as a sole carbon source, a likely product of ethanol oxidation (Fig. 9A).[69] We could further show that not only *madA* but also the mycofactocin biosynthesis is upregulated in *M. smegmatis* on ethanol *versus* glucose as the sole carbon source[53] and also that acetate accumulates in liquid medium when grown on ethanol.[41] These results led to the proposed mycofactocin-dependent ethanol utilization pathway depicted in Fig. 9A. Accordingly, ethanol is oxidized by *madA* to acetaldehyde in an MFT-dependent dehydrogenation reaction, followed by a second oxidation step from acetaldehyde to acetate by an as-yet unidentified acetaldehyde dehydrogenase. One candidate for the elusive acetaldehyde dehydrogenase could be the zinc-dependent aldehyde dehydrogenase MscR (MSMEG_4340). It was shown to be able to oxidize formaldehyde, acetaldehyde, and propionaldehyde *in vitro* and is upregulated under aldehyde stress.[70,73] However, MscR is merely one candidate of more than 50 putative aldehyde dehydrogenases encoded in the genome of *M. smegmatis* mc^2 155. Whether the acetaldehyde oxidation is mycofactocin-dependent remains to be elucidated. The following acetate utilization, however, is not strictly mycofactocin-dependent as demonstrated by mycofactocin biosynthesis gene knock-outs able to grow on acetate as the sole carbon source.[69]

5.2 The mycofactocin-dependent alcohol degradation gene cluster

MadA from *M. smegmatis* mc^2 155 (MSMEG_6242, Table 2) was not only indirectly shown to be involved in the utilization of short-chain primary alcohols. It was also directly demonstrated *in vitro* to possess primary alcohol (C1–C4) dehydrogenase as well as formaldehyde dismutase activities in the presence of the artificial electron acceptor *N*,*N*-dimethyl-*p*-nitrosoaniline (NDMA).[51] In *M. smegmatis*, *madA* is encoded in a putative gene cluster comprising the genes MSMEG_6236-6242. Interestingly, this gene cluster is located directly upstream of *mftM*, to which, as outlined in chapter 4.2, *madA* is tightly linked *via* strict co-occurrence in a genome-wide context. It should be noted that these two genes are not always encoded in the same locus, albeit encoded in the same genome (Fig. 5A). The genes included in the MSMEG_6236-6242 cluster, despite MSMEG_6242, are MSMEG_6239 (*madD*) – a putative IPR001670-family 1,3-propandiol dehydrogenase, MSMEG_6240 – a putative von Willebrand factor type A (VWA) domain (PF05762)-containing protein of unknown function, MSMEG_6241 – a putative MoxR-type AAA+ ATPase domain (PTHR42759)-containing protein of unknown function, and MSMEG_6236 (*madR*)/MSMEG_6238 (*madS*) – a two-component system regulating the expression of MSMEG_6239 and MSMEG_6242 in the presence of methanol, 1,3-propandiol, and under starvation conditions, *i.e.* absence of a carbon source.[39,40] MSMEG_6240 and MSMEG_6241 might be involved in maturation of MSMEG_6239 and MSMEG_6242,

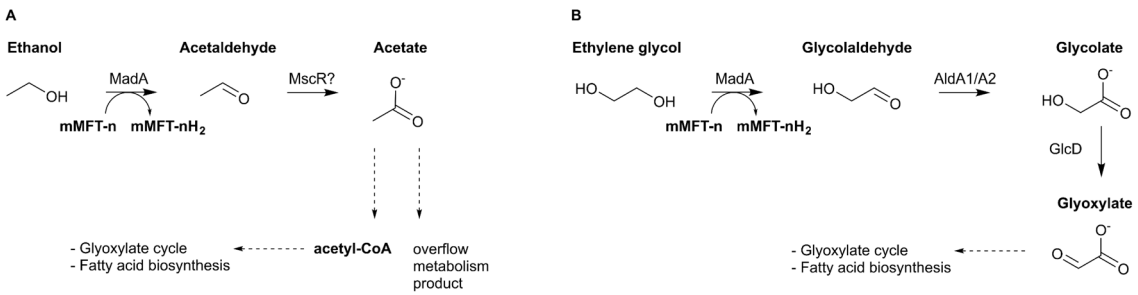

Fig. 9 Hypothesized mycofactocin-dependent *mad*-mediated alcohol utilization pathways. (A) Proposed ethanol assimilation pathway in *M. smegmatis*. Ethanol is oxidized to acetaldehyde in an MFT-dependent reaction by MadA (A0R5M3, MSMEG_6242) and further oxidized to acetate by an unknown acetaldehyde dehydrogenase, potentially MscR (A0R0C7, MSMEG_4340).[69,70] The acetate might either be excreted as an overflow metabolite[71] or further metabolized *via* acetyl-CoA. (B) Proposed and simplified ethylene glycol assimilation pathway for *R. jostii* RHA1. Ethylene glycol is oxidized in a mycofactocin-dependent reaction by MadA (Q0S3Q2, RHA1_ro06057) followed by oxidation of the resulting glycolaldehyde to glycolate by AldA1 (Q0S3M8, RHA1_ro06081) and/or AldA2 (Q0RXM5, RHA1_ro08917) and further to glyoxylate by GlcD (Q0SBQ6, RHA1_ro03227). Glyoxylate might be further metabolized *via* the glyoxylate shunt.[59,72] mMFT-*n* – methylmycofactocinone-*n*, mMFT-*n*H$_2$ – methylmycofactocinol-*n*, MadA – mycofactocin-dependent alcohol dehydrogenase, MscR – *S*-nitrosomycothiol reductase MscR, AldA1 – aldehyde dehydrogenase A1, AldA2 – aldehyde dehydrogenase A2.

Table 2 Gene names and locus tags of the *mad* cluster of *R. jostii* RHA1 (*mad* convention) and their corresponding homologs in *M. smegmatis* mc^2 155. *madA* – mycofactocin-dependent alcohol dehydrogenase, *madB* – MoxR-type AAA+ ATPase, *madC* – VWA domain-containing protein, *madD* – putative mycofactocin-dependent 1,3-propanediol dehydrogenase, *madS* – mad-cluster sensor histidine kinase, *madR* – mad-cluster response regulator transcription factor

R. jostii RHA1 gene name (locus)	*M. smegmatis* mc^2 155 gene name (locus)
madA (RHA1_ro06057)	*mno*/*mdo* (MSMEG_6242)
madB (RHA1_ro06058)	MSMEG_6241
madC (RHA1_ro06059)	MSMEG_6240
madD (RHA1_ro06060)	MSMEG_6239
madS (RHA1_ro06061)	*mnoS* (MSMEG_6238)
madR (RHA1_ro06062)	*mnoR* (MSMEG_6236)

which is most likely dependent on cations as described in chapter 6.3. Notably, MoxR-type ATPase domain proteins are known to co-occur and co-locate with VWA-domain proteins[74] and can act as chaperones aiding in the maturation of metal-dependent proteins, *e.g.* during the insertion of non-heme iron.[75] Two independent studies recently discovered a gene cluster homologous to the *M. smegmatis* MSMEG_6236-6242 cluster in *R. jostii* RHA1,[59,72] where it is involved in ethylene glycol catabolism. Roccor *et al.* demonstrated that an *R. jostii* RHA1 Δ*madA* strain failed to utilize ethylene glycol as the sole carbon source and the wildtype was shown to convert ethylene glycol to glycolaldehyde (Fig. 9B).[72] These results suggest that the MSMEG_6242 cluster and homologs thereof confer mycofactocin-dependent alcohol utilization capabilities which therefore were named mycofactocin-dependent alcohol degradation (*mad*) pathway. Thus, the MSMEG_6236-6242 cluster and homologous gene clusters are further addressed in the naming convention proposed by Roccor *et al.* as the *madABCDSR* cluster.[72] Table 2 provides an overview of the *M. smegmatis* mc^2 155 and *R. jostii* RHA1 *mad* gene clusters with gene names and linked loci as depicted in Fig. 5A. In the system of *R. jostii*, two aldehyde dehydrogenases were proposed to convert glycolaldehyde to glycolate, AldA1 (RHA1_ro06081/RHA1_RS29725) and AldA2 (RHA1_ro08917/RHA1_RS39755).[72] Both do not share sequence homology with MSMEG_4240 (MscR).

In summary, the evidence suggests that one of the physiological roles of mycofactocin in mycofactocin methylating strains, encoding *mftM* in combination with the *mad* gene cluster, is the oxidation of short-chain alcohols, such as ethanol. Mycofactocin supposedly acts as an external electron acceptor for the non-exchangeable nicotinamide adenine dinucleotide (phosphate) of *madA* (and potentially MadD) as outlined in Fig. 8.

5.3 The physiology of *mftM*-negative mycofactocin producers

In contrast to the mycofactocin-dependent ethanol utilization in mycofactocin methylating strains, little is known about the physiological role of mycofactocin in non-methylating strains, such as *M. tuberculosis* H37Rv. Mycofactocin methylating strains maintain the ability to grow on ethanol as the sole carbon source when *mftM* is knocked out, albeit with a longer lag phase, as demonstrated for *M. smegmatis*.[54]

Notably, non-methylating strains systematically lack the *madA* gene and therefore also the alcohol utilization pathways proposed in Fig. 9. This suggests the existence of an alternative, yet unknown, ethanol assimilation pathway in these strains. *M. marinum*, a species of the non-methylating group, was shown to grow on ethanol as the sole carbon source.[69] Growth was inhibited when *mftD* was deleted, indicating that the ethanol utilization in *M. marinum* is MFT-dependent. A second line of evidence for an alternative *madA*-independent ethanol degradation pathway involves *M. tuberculosis* H37Rv. Here, the maximum cell density *in vitro* was halved when grown on ethanol and cholesterol as carbon sources upon deletion of *mftD*.[69] Notably, Daniel Haft identified three and nine potential mycofactocin-dependent oxidoreductases in *M. tuberculosis* H37Rv and *M. marinum* strain M, respectively.[31] These data sets indicate the presence of a *madA*-independent but mycofactocin-dependent ethanol utilization pathway in this group of mycofactocin producing organisms. Besides alcohol utilization, mycofactocin might also play a role in the biosynthesis of the cell wall of these strains as we will describe in chapter 6.2.

5.4 Regulation of mycofactocin biosynthesis

In the previous chapters, we described how mycofactocin is involved in the short chain alcohol metabolism of bacteria and how mycofactocin biosynthesis is elevated upon presence of different alcohols such as ethanol or ethylene glycol. However, not only alcohols but also oxygen appears to play a role in the regulation of mycofactocin biosynthesis. It was shown that the expression levels of the mycofactocin biosynthesis genes *mftC* and *mftD* are highly increased in low oxygen conditions in *M. tuberculosis*.[76] This trend is supported by findings for *M. smegmatis* where elevation in mycofactocin biosynthesis correlated with decreasing oxygen transfer rates in liquid culture.[71] Proteome data for *M. tuberculosis* during *in vitro* dormancy, a state of survival induced by low oxygen availability, showed increased MftD levels.[77] The increased expression of *mftD* under low oxygen conditions might be a compensation mechanism for its oxygen-dependency, as the MftD reaction consumes one oxygen molecule (Fig. 7). Another reason for the increased mycofactocin biosynthesis during low oxygen conditions might be an increased reliance of the bacteria on energy gained through mycofactocin-dependent substrate oxidation pathways. For example, ethanol oxidation *via* acetaldehyde to acetate as

proposed in Fig. 9A could be such an energy source. This hypothesis is supported by data for *M. smegmatis* where increasing mycofactocin concentrations correlated with increasing acetate concentrations in ethanol-containing liquid medium upon lowering oxygen availability.[71] Thus, the energy and carbon metabolism under low O_2 conditions appear to be fuelled mostly by the first steps of ethanol oxidation instead of downstream acetate utilization, potentially necessitated by a reduced proton gradient-driven ATP generation as an effect of the lower oxygen availability.

Mycofactocin biosynthesis is induced by short-chain primary alcohols and low oxygen concentration. However, the molecular regulatory network behind this induction is unknown. The mycofactocin biosynthetic gene cluster *sensu latu* not only includes the genes *mftABCDEF(M)* but also *mftR*, encoding the transcriptional regulator MftR. As depicted in Fig. 5A, the regulator is usually encoded upstream of *mftA* in reverse orientation and has been shown to recognize a palindromic sequence upstream of the *mftA* gene (5′-T-N_2-GGCA-N_5-TGCC-N_2-A-3′) acting as a transcriptional repressor for *mftA* in dimeric form.[78] Despite all metabolic evidence presented so far pointing towards a function of mycofactocin in alcohol utilization, it was shown that MftR binds long-chain acyl coenzyme A esters (acyl-CoA), particularly oleoyl-CoA. Binding of ligand induces a confirmational change in the MftR dimer leading to dissociation of the repressor from the bound DNA, resulting in derepression of the mycofactocin BGC.[78,79] A direct link between the induction of mycofactocin biosynthesis by ethanol or low oxygen conditions, and derepression of mycofactocin biosynthesis by binding long-chain acyl-CoA to MftR remains to be established. In chapter 6 we will examine how not only the MFT biosynthesis but also the expression of potentially mycofactocin-dependent enzymes is induced upon presence of ethanol and a variety of other molecules (overview presented in Fig. 10).

6. Mycofactocin-dependent dehydrogenases

Chapter 2 introduced the mycofactocin BGC to be co-occurring with originally three families of putatively mycofactocin-dependent oxidoreductases postulated to use the redox cofactor to reoxidize their internal non-exchangeable NAD(P)H (Fig. 8 and Table 1). These were the short-chain dehydrogenase family *SDR_subfam_1* IPR023985, the putatively zinc-dependent alcohol dehydrogenase family IPR023921 (*ADH_Zn_actinomycetes*), and lastly the divalent cation-dependent alcohol dehydrogenase family IPR001670, whose members were not exclusively associated with the mycofactocin BGC as it represents a superfamily with members from the bacterial and fungal kingdom.[31] Since this first study in 2011, additional putatively mycofactocin-dependent protein families were defined *via* hidden Markov models (HMMs) including the 4-nitroso-*N*,*N*-dimethylaniline (*NDMA*)-dependent methanol dehydrogenase family IPR026338 (*NDMA_methanol_DH*), the two conserved hypothetical protein (CHP) families CHP03977 and CHP03996, and the short-chain dehydrogenase families *SDR_subfam_2*, *SDR_subfam_3*, and *SDR_subfam_4* (InterPro version 104.0).[35,80] Currently, no experimental data is available for any member of these newly defined families, except for *NDMA_methanol_DH*. However, several members of the originally proposed families and of IPR026338 *NDMA_methanol_DH* were experimentally investigated, albeit almost exclusively with artificial electron acceptors.

6.1 The short-chain dehydrogenase family IPR023985

One family of oxidoreductases that was shown to genomically co-occur with the mycofactocin cluster is the *SDR_subfam_1* IPR023985. The first studied member of this family, and to date the only biochemically characterised enzyme of this group, is the carveol dehydrogenase LimC from *R. erythropolis* DCL14

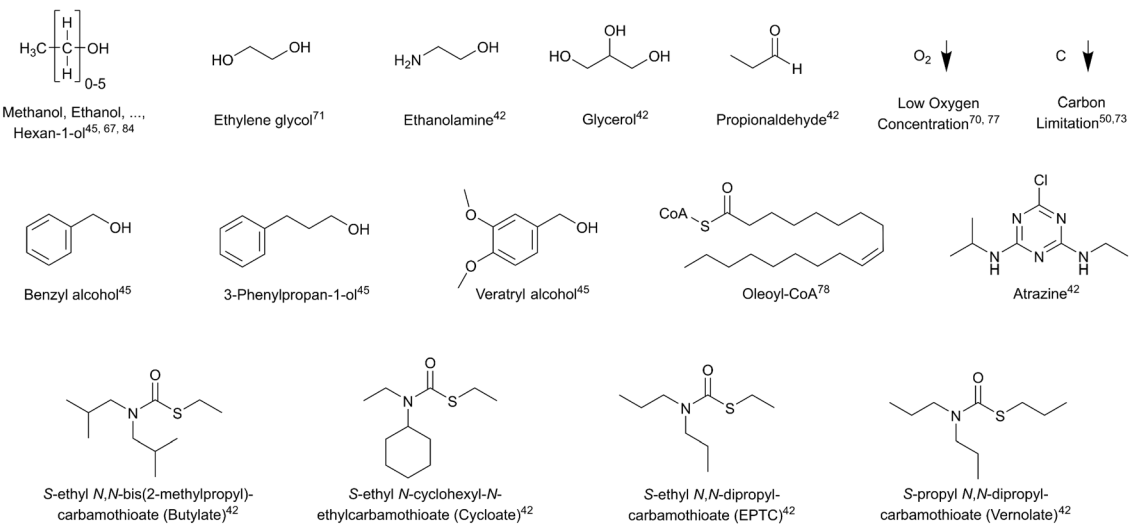

Fig. 10 Mycofactocin-system inducing agents. The listed molecules and conditions were shown to induce either mycofactocin biosynthesis directly or to induce the expression of putatively mycofactocin-dependent enzymes. The list is not exhaustive but comprises major classes of reported inducing agents, such as linear primary alcohols, secondary alcohols, aldehydes, thiocarbamates and acyl-CoA esters. CoA – coenzyme A.

(UniProt: Q9RA05). It was shown to bind one NAD(H) molecule per subunit of its homotetramer, but does not bind metal ions (Fig. 11A).[43] The enzyme catalyses oxidation of L-carveol to L-carvone, the first step of a proposed limonene degradation pathway of *R. erythropolis* DCL14, hence LimC.[82] However, this reaction was conducted with an artificial external electron acceptor, 2,6-dichlorophenol indophenol (DCPIP), *in vitro*, with the natural redox partner remaining unknown at the time. Already in this study by van der Werf *et al.* from 1999 it was proposed that the internal NAD(H) is hindered from diffusing out of the protein by a ten amino acid long insertion loop located on primary sequence level towards the N-terminus and adjacent to the NAD(H) cofactor insertion site.[43] These results were supported by a crystallography study conducted on other mycobacterial members of the IPR023985 *SDR_subfam_1* family which showed non-exchangeable binding of NAD(H) coordinated by the insertion loop as proposed for LimC (Fig. 11B) but also a second disordered loop located towards the C-terminus of the proteins, which together almost entirely bury the cofactor inside each subunit of the homotetramer.[42]

First evidence for an interaction of mycofactocin with a putatively mycofactocin-dependent dehydrogenase of *SDR_subfam_1* was presented for the LimC homolog MSMEG_1410 (UniProt: A0QSA5) from *M. smegmatis* mc^2 155

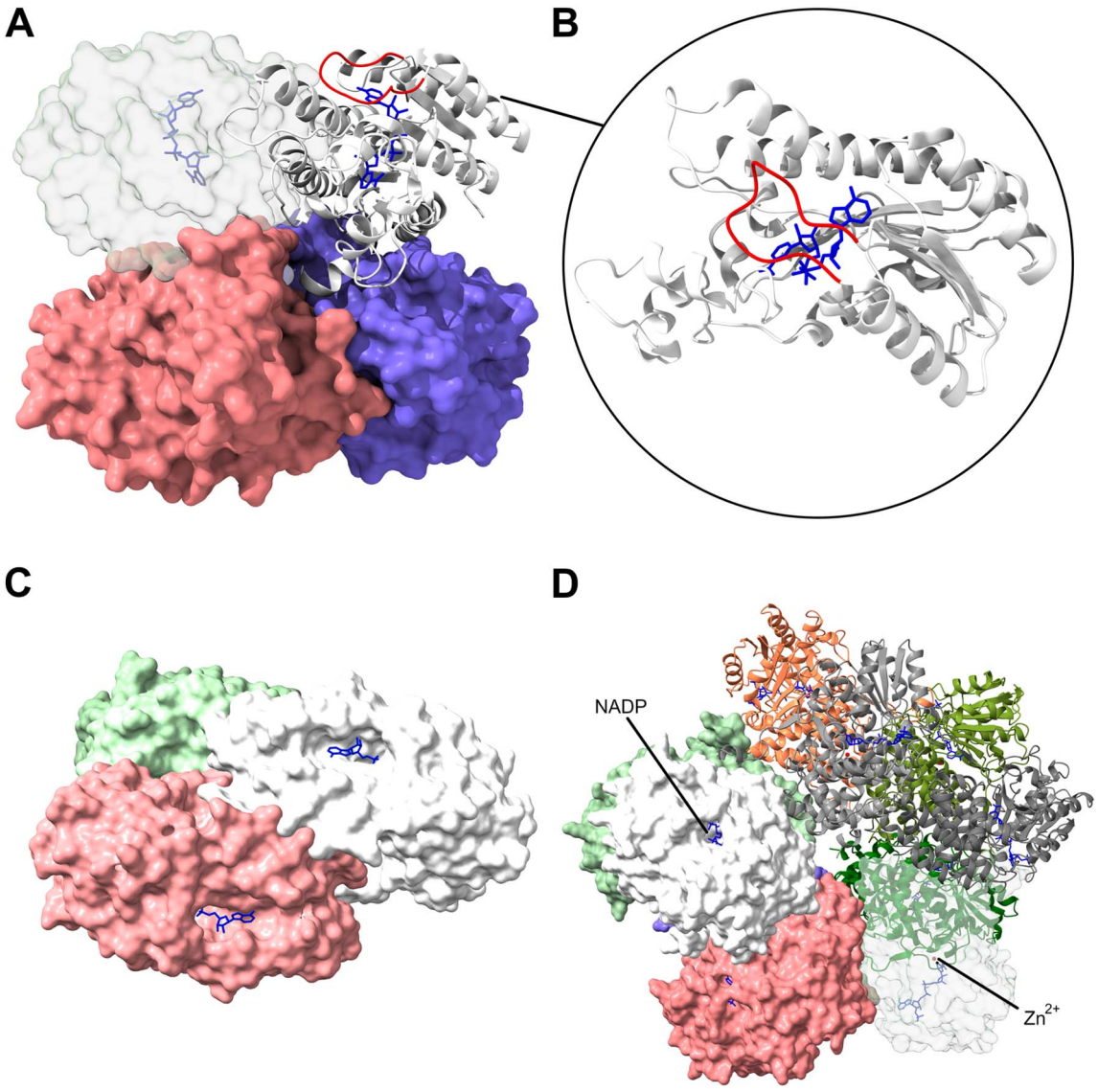

Fig. 11 Protein structures of studied mycofactocin-dependent dehydrogenases. (A) Shows the crystal structure of the homotetrameric structure of the putative carveol dehydrogenase B1MLR7 (PDB: 3S55) from *Mycobacteriodes abscessus* belonging to the *SDR_subfam_1* family with one subunit depicted in detail in (B).[42] The insertion loop hindering the internal NAD(H) from diffusing, here ENSDVVGYPLA (amino acids 41–51), is highlighted in red for this subunit. (C) Structural model of the homotrimeric NDMA-dependent alcohol dehydrogenase P80175 from *Amycolatopsis methanolica* 239 belonging to the IPR023921 *ADH_Zn_actinomycetes* family. (D) Structural model of the decameric NADP(H)-binding NDMA-dependent alcohol dehydrogenase Q9RCG0 from *A. methanolica* 239 closely resembling the reported electron micrographs of this five-fold symmetric decameric enzyme as shown by Bystrykh *et al.* which belongs to the *NDMA_methanol_DH* family IPR026338 with Zn^{2+} ions highlighted in red.[49] Typically, 1–2 zinc and magnesium ions and one NADP(H) are bound per subunit. All cofactors are buried deeply within the structure. The NAD(P) cofactors are highlighted in blue for all structures. Structure models C and D were constructed using AlphaFold 3.[81]

which was shown to reduce the mycofactocin aglycon MFT-0 during carveol oxidation to MFT-0H_2 *in vitro*.[37] Similarly, heterologously produced LimC from *R. erythropolis* DCL14 reduced all observable mycofactocin species, including glycosylated congeners, present in metabolome extracts of *M. smegmatis* when carveol was offered as a substrate.[53] However, kinetic studies with pure cofactors, particularly mycofactocins with defined glycosyl side chains, are missing to date, as well as a crystal structure showing the interaction of *SDR_subfam_1* enzymes with the mycofactocin cofactor. This is true for all putatively mycofactocin-dependent enzymes described in this chapter.

6.2 The putatively zinc-dependent dehydrogenase family IPR023921

The second originally proposed protein family associated with the mycofactocin BGC is the family of putatively zinc-dependent alcohol dehydrogenases IPR023921 *ADH_Zn_actinomycetes*.[31] Within this family, one enzyme from *Amycolatopsis methanolica* 239 (UniProt: P80175) and one from *Rhodococcus opacus* DSM 1069 (UniProt: P81747) have been studied *in vitro*. The former was shown to be a homotrimeric, the latter to be a homotetrameric alcohol dehydrogenase with one NAD(H) bound per subunit (Fig. 11C). *In vitro*, the enzymes exhibited NDMA-dependent dehydrogenase activities towards a wide range of alcohols, such as ethanol, propan-1-ol, and butan-1-ol, up to octan-1-ol, but also isobutanol, cyclohexanol, benzyl alcohol, vanillyl alcohol, or 3-phenylpropan-1-ol,[47] which also induced expression of their genes.[46] These enzymes, unlike those of the *NDMA_methanol_DH* family, did not display methanol dehydrogenase, nor aldehyde dismutase or aldehyde reductase activities. Despite different primary structures as well as higher-order structures, this family shares key similarities with enzymes from the *SDR_subfam_1* family in that it contains one non-exchangeable NAD(H) per subunit and oxidizes alcohol groups in dehydrogenation reactions dependent on an external redox molecule.

Another putative dehydrogenase of this family, Rv3086 (UniProt: P9WQB9), encoded in the genome of *M. tuberculosis* H37Rv, appears to play a role in the biosynthesis of the mycobacterial cell wall, specifically in the biosynthesis of mycolic acids as part of the *mymA* operon (Rv3083–Rv3089). This operon is induced under acidic conditions and during infection of macrophages. Disruption of the *mymA* operon and its regulation resulted in a reduced bacterial infection load in guinea pig spleens as well as a higher susceptibility to antimycobacterial drugs. However, no function could be attributed to this gene so far.[83] All three studied proteins of this family were not investigated regarding their metal content and dependencies. Thus, it remains to be elucidated whether this family is zinc dependent as inferred from sequence homology.[46]

6.3 NDMA-dependent methanol dehydrogenase family IPR026338

The last family of experimentally investigated enzymes of the potentially mycofactocin-dependent alcohol dehydrogenase families is the *NDMA_methanol_DH* family IPR026338, with one prominent example being the methanol:NDMA oxidoreductase Q9RCG0 (UniProt) from *A. methanolica* 239 (previously known as Mno), which is one of the defining members of this enzyme family while it also appears to be part of the divalent cation-dependent IPR001670 superfamily. This enzyme, along with an apparent homolog from *Mycobacterium gastri* MB19, was shown to be a homodecamer, binding non-exchangeable NADP(H) and containing Mg^{2+} and Zn^{2+} ions (Fig. 11D).[49] Both enzymes were further shown to possess dehydrogenase capabilities for a wide range of alcohols, such as methanol, ethanol, or butan-1-ol, but also ethylene glycol or isobutanol. Interestingly they also possess formaldehyde dismutase and NADH-dependent primary aldehyde (C1–C4) reductase activities.[48,84] In the methylotrophic *Mycobacterium* sp. JC1, a similar protein, C5MRT8 (UniProt), was identified, which exhibited NDMA-dependent dehydrogenase activities for methanol, ethanol, and formaldehyde but not for propan-1-ol or butan-1-ol. The protein was further shown to be essential for growth on methanol as the sole carbon source in this strain.[50] Another member of this family, ThcE (UniProt: Q53062), was found in *R. erythropolis* NI86/21, which showed an NDMA-dependent methanol dehydrogenase activity and was expressed upon presence of herbicides such as atrazine or the thiocarbamates *S*-ethyl dipropylcarbamothioate (EPTC) and vernolate but also ethanolamine or ethanol as carbon sources (Fig. 10).[44,85] In this strain, the enzyme appears to be part of a cytochrome P450 system involved in the degradation of these herbicides.[86] During the herbicide degradation process, aldehydes like propionaldehyde in case of EPTC are formed,[83] which hypothetically could be metabolized by ThcE in aldehyde dismutase or reductase reactions as shown for its homologs from *A. methanolica* and *M. gastri* described above. Furthermore, a member of this family from *R. erythropolis* N9T-4 (UniProt: A5LHA1) was shown to be highly induced under oligotrophic conditions, surprisingly together with an NAD-dependent formaldehyde dehydrogenase (UniProt: A5LHA2). The latter is a homolog of the proposed aldehyde dehydrogenases AldA1 (Q0S3M8) and AldA2 (Q0RXM5) of *R. jostii* RHA1, potentially involved in glycolaldehyde oxidation (Fig. 9B), exhibiting 95% primary sequence identity to both proteins. This *NDMA_methanol_DH* family member of *R. erythropolis* N9T-4 (A5LHA1) exhibited formaldehyde dismutase activity as shown for its homologs described above.[52] Intriguingly, also *madA* from *R. jostii* RHA1 (UniProt: Q0S3Q2) and *M. smegmatis* mc^2 155 (UniProt: A0R5M3) belong to the *NDMA_methanol_DH* family, which, as outlined above, are involved in the oxidation of ethylene glycol and ethanol, respectively.[59,69,72] *madA* from *M. smegmatis* mc^2 155, besides its ethanol dehydrogenase activity, was also shown to possess dehydrogenase activities for methanol, propan-1-ol, butan-1-ol, and NADH-dependent reductase activity towards their corresponding aldehydes *in vitro* and was shown to be required for growth of the strain on methanol as the sole carbon source.[51] The enzyme was further demonstrated to possess NADH- but not NADPH-dependent aldehyde reductase activity as known for the homologs from *M. gastri* and *A. methanolica*.[87] Overall, it appears that MadA and its homologs of the *NDMA_methanol_DH* family are dependent on divalent cations, use

NADP(H) as an internal non-exchangeable cofactor and accept a wide range of rather short-chained alcohols in dehydrogenation reactions but might also contribute to the detoxification of aldehydes *via* aldehyde dismutase and reductase activities. However, a direct interaction of these enzymes with mycofactocin remains to be investigated as all studies on these enzymes used the artificial electron acceptors NDMA or DCPIP instead of their elusive *bona fide* electron acceptor, which likely is mycofactocin.

In summary, all mycofactocin-dependent alcohol dehydrogenase families studied so far share certain characteristics such as the dependence on an external redox cofactor, most likely mycofactocin, as well as the use of a non-exchangeable nicotinamide during the dehydrogenation reaction. However, the three families also exhibit clear differences, which can be summarized as follows: (1) *SDR_subfam_1* – metal-independent homotetrameric NAD(H)-binding short chain alcohol dehydrogenases described by IPR023985, (2) *ADH_Zn_actinomycetes* – NAD(H)-employing dehydrogenases with a broad alcohol substrate spectrum described by IPR023921, and (3) *NDMA_-methanol_DH* – divalent cation-dependent homodecameric and NADP(H)-utilizing alcohol dehydrogenases, with a potential secondary function as aldehyde dismutase and reductase, described by IPR026338. Enzymes of these three families appear to be involved in a wide range of pathways for alcohol utilization but also seem to play a role during cell wall biosynthesis and might even be indirectly involved in carbon fixation as proposed by Ohhata *et al.* for *R. erythropolis* N9T-4.[52] Proteins of this group of potentially mycofactocin-dependent enzyme families thereby mediate a high metabolic flexibility and stress resistance enabling their cognate hosts to thrive in versatile environments. Future studies will have to investigate a direct interaction between the enzymes and their presumable redox cofactor mycofactocin as well as experimentally characterize members of the recently defined putative mycofactocin-dependent enzyme families described in the introduction of chapter 6.

7. The role of mycofactocin in respiration

With the substrate oxidation side of the mycofactocin energy conservation landscape covered, we need to take a closer look at how reoxidation of mycofactocinols, *i.e.* (m)MFT-*n*H_2 to mycofactocinones, *i.e.* (m)MFT-*n*, is achieved. First, we will revisit the electron flow in PQQ systems, to which the mycofactocin system appears to be functionally related. Subsequently, we will propose a hypothetical scheme of electron flow from ethanol *via* mycofactocin to a terminal electron acceptor and discuss, how the reoxidation of accumulated mycofactocinols could be coupled with energy conservation in the electron transport chain (ETC).

7.1 The electron flow in PQQ systems

Acetic acid bacteria utilizing PQQ-dependent alcohol dehydrogenases demonstrate additional entry points for electrons into the ETC. Besides the classical bacterial ETC, comprising an NADH-dehydrogenase, a quinone pool, a terminal oxidase and an ATP synthase, located in the cell membrane, acetic acid bacteria possess a so-called oxidative fermentation pathway. In this pathway, PQQ-dependent dehydrogenases, located in the periplasmic space and the cell membrane, obtain electrons from reduced substrates such as ethanol or glucose. During the reaction, the PQQ cofactor, a prosthetic group of the same enzyme, is reduced to $PQQH_2$. The cofactor is subsequently reoxidized to PQQ by cytochrome *c* subunits that facilitate electron transfer to the ubiquinone pool.[9] The reduced ubiquinols are reoxidized by a terminal oxidase – ubiquinol oxidase – thereby contributing to the proton motive force, which is harnessed by ATP synthase to generate ATP (Fig. 1).[9] Thus, the PQQ system allows for an additional electron entry point besides the classical NADH-dehydrogenase for electron shuttling from alcohols directly to the quinone pool.

7.2 MftG is involved in the electron transfer from mycofactocinol to the electron transport chain

In the mycofactocin system, MFT is supposed to serve as a freely diffusible electron acceptor of primary dehydrogenases. However, the cofactor reoxidation step would require an additional enzyme or subunit that would reoxidize mycofactocin, potentially transferring the electrons to the ETC. This enzyme remained unknown until we recently investigated *mftG*, a previously uncharacterized gene encoded in the majority (*ca.* 75%) of mycofactocin BGCs (Fig. 5A).[41] Its gene product is a flavoenzyme belonging to the superfamily of the glucose–methanol–choline (GMC) oxidoreductases.[88] Our recent observations demonstrated that deletion of the *mftG* gene (MSMEG_1428) in *M. smegmatis* resulted in a growth defect on ethanol as a sole carbon source, comparable to the phenotype of a mutant deficient in mycofactocin biosynthesis on ethanol. Moreover, Δ*mftG* cells demonstrated a starvation phenotype inferred from an ADP/ATP ratio evaluation, and a differential transcriptomic analysis of *M. smegmatis* cells lacking the *mftG* gene revealed a dramatic reorganization of the ETC.[41,89] Strikingly, metabolome analyses revealed that Δ*mftG* mutants accumulated reduced mycofactocin species, pointing towards impaired cofactor reoxidation as a cause of the growth deficit. Indeed, experiments using isolated mycobacterial membranes from *M. smegmatis* wildtype, incubated with either MFT-0H_2 or mMFT-2H_2, demonstrated stimulation of respiration. Membranes isolated from the corresponding Δ*mftG* strain did not show a comparable respiration rate. These findings were corroborated by LC-MS analyses of the incubated membranes exhibiting indeed an oxidation of mycofactocinols by wildtype membranes. This suggested that MftG is involved in the electron transfer from mycofactocinols to the ETC of mycobacteria as depicted schematically in Fig. 12. The direct interaction of MftG with mycofactocin was further shown by cell-free enzymatic assays with semi-purified MftG that promoted conversion of MFT-0H_2 and mMFT-2H_2 into their respective oxidized forms. These experiments showed the ability of MftG to interact with and reoxidize reduced mycofactocins. However, the particular electron acceptor of MftG and the entry point of the

electrons into the respiratory chain, *i.e.* the quinone pool or cytochromes, remain unclear. In conclusion, a hypothetical mycofactocin-dependent energy conservation pathway would follow the scheme outlined in Fig. 12.

7.3 A comparison of the electron flow in PQQ and mycofactocin systems

As described above, mycofactocin serves as the redox cofactor transferring electrons from alcohols to the mycobacterial ETC in a similar fashion as PQQ serves as a redox cofactor in alcohol oxidation pathways of acetic acid bacteria. The reduced $PQQH_2$ is oxidized by the cytochrome *c* subunits of PQQ-dependent dehydrogenases using ubiquinone as the electron acceptor, thus functioning as an entry point into the ETC. Mycofactocin, however, appears to require the activity of MftG for its reoxidation, a flavoprotein that delivers electrons to an unknown acceptor, most likely menaquinones or cytochromes. One important difference between the two cofactors is that PQQ is tightly bound to its enzymes, thus acting as a prosthetic group, while mycofactocin is a diffusible molecule, acting as a co-substrate. The redox cofactor thus represents an integrating redox pool for reducing equivalents originating from a variety of MFT-dependent dehydrogenation reactions, as demonstrated

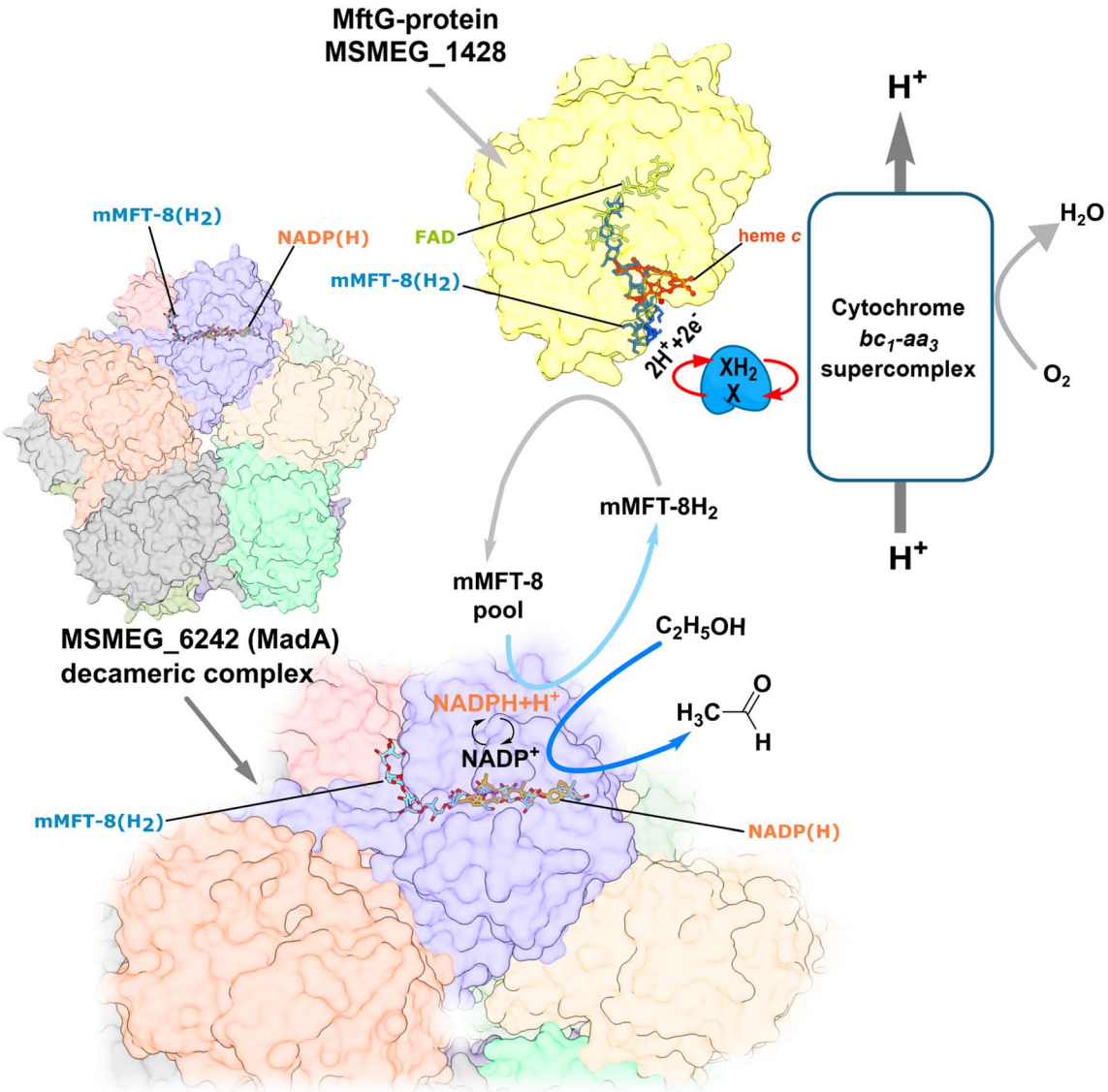

Fig. 12 Hypothetical mycofactocin-mediated electron shuttling pathway. Alcohol oxidation is performed by mycofactocin-dependent alcohol dehydrogenase (MadA, MSMEG_6242). This protein represents a decameric complex – AlphaFold 3 prediction of the structure is shown. Autodock Vina[90] was used for visualisation of NADPH binding to the internal pocket of one subunit (coloured in yellow). Similarly, docking of mMFT-$8H_2$ was performed (sky blue); the binding mode of cofactors is an illustration only and requires experimental confirmation. Reoxidation of the reduced MFT-molecules is performed by MftG (MSMEG_1428). Docking of FAD (green) and mMFT-$8H_2$ (dark blue) to the receptor is shown (AlphaFold 2 structural prediction). The binding of a heme *c* (red) can be similarly expected. A further interaction partner of MftG remains unknown, but a flow of electrons to the mycobacterial ETC through the menaquinone pool (MQ/MQH_2) may be hypothesised.

e.g. by the oxidation of ethanol and carveol. This system, as opposed to the prosthetic PQQ system, might circumvent the necessity for MFT-dependent dehydrogenases to carry an additional dedicated subunit for coenzyme reoxidation. Instead, the mobile coenzyme may diffuse freely towards MftG, which thus bundles electrons from several MFT-dependent primary oxidases.

8. Open questions and future directions

This review provides a comprehensive overview of mycofactocin research, tracing its progression from initial bioinformatic predictions to its discovery *in vivo*. The biosynthetic pathways and chemical synthesis strategies for mycofactocin were discussed in detail and recent biological advances, including the elucidation of an MftG-mediated electron transfer pathway linking mycofactocin to the mycobacterial respiratory chain, were highlighted. Over the past 14 years, experimental efforts have established mycofactocin as a redox cofactor with intriguing parallels to PQQ. These peculiar similarities comprise a biosynthesis *via* RiPP pathways involving rSAM-mediated cyclization reactions as well as an involvement in electron transfer during aerobic alcohol metabolism. In the absence of (detectable) shared ancestry of most enzymes involved in each biosynthetic system, a common ancestry of the PQQ and mycofactocin systems, which are predominantly found in Gram-negative and Gram-positive bacteria, respectively, is unlikely. Therefore, the two cofactors might represent an extraordinary example of parallel evolution. Besides the obvious selective pressure to evolve alternative hydride carriers, the fundamental question remains: what biological advantage is conferred by their production? Besides an optimized redox potential, alternative cofactors might offer more flexibility, in particular independence of the NAD(H) pool as well as alternative regulation and localization. It also remains open whether further examples of as-of-yet uncharacterized peptide-derived cofactors exist.

Looking at the mycofactocin system in particular, several critical questions remain unanswered, presenting excellent opportunities for future research. In recent years, mycofactocin-dependent alcohol oxidation reactions were investigated both *in vivo* and *in vitro*. However, the direct mode of interaction between the protein and the mycofactocin molecules remains to be investigated. Future studies will have to focus on in-depth biochemical investigation using purified enzymes and cofactors as well as crystallographic studies of mycofactocin-dependent dehydrogenases in complex with their cofactor. Attention should be given to the difference between methylated and non-methylated mycofactocins and structural studies will need to define the cofactor's absolute stereochemistry. These experiments should be accompanied by synthetic approaches to the different stereoisomers, followed by thorough biochemical characterization and comparison.

Another important task will be to find the exact electron transfer pathway from mycofactocinol to a terminal electron acceptor during energy conservation. Moreover, future investigation is necessary on how a lack of MftG is compensated in organisms not encoding a member of this protein family. It was speculated that enzymes of related families could be able to act in replacement of MftG but no functional homolog has been found so far. Another prospect is the experimental search and investigation of predicted and potentially undiscovered mycofactocin-dependent enzymes through approaches such as chemical proteomics or classical activity-guided protein purification. Such dehydrogenases might be useful for specific alcohol oxidation reactions, as demonstrated for the stereoselective conversion of L-carveol to L-carvone by LimC, and might turn out valuable for synthetic biology approaches to increase the substrate spectrum of naturally mycofactocin-negative organisms. It could be envisioned, for example, to degrade environmentally critical plastic waste like polyethylene terephthalate (PET) *via* PET hydrolases to ethylene glycol as one main product[91] and subsequently use ethylene glycol dehydrogenases as proposed by Roccor *et al.* to fuel the bacterial carbon and energy metabolism to biologically produce compounds of interest in bacterial hosts.[72]

Not only biotechnological use cases are possible. As seen in Chapter 6.2, mycofactocin may also play a critical role in the mycobacterial cell wall biosynthesis through involvement in the cell wall biosynthesis-related *mymA* operon in *M. tuberculosis* H37Rv, making it a potential target for infection and antibiotic research to find new ways to fight infections caused by this pathogenic species. A related example for an antimycobacterial agent linked to cofactor metabolism is the prodrug pretomanid, which is activated by a coenzyme-F_{420}-dependent oxidoreductase. The activation reaction transforms the compound into a molecule that subsequently impairs the mycobacterial cell wall biosynthesis thereby reducing its fitness under infection conditions.[92]

In summary, mycofactocin not only provides an interesting landscape for academic research in the fields of microbiology and biochemistry but also has the potential to serve in biotechnological approaches and potentially in the development of novel antimycobacterial drugs.

9. Data availability

No primary research results, software or code have been included and no new data were generated as part of this review.

10. Conflicts of interest

There are no conflicts to declare.

11. Acknowledgments

W. K. A-J. thanks the German Academic Exchange Service (DAAD) for a graduate fellowship. L. G. thanks the State of Thuringia for a graduate fellowship (Landesgraduiertenstipendium). Funded by the Open Access Publishing Fund of the University of Bayreuth.

12. References

1 C. Andreini, I. Bertini, G. Cavallaro, G. L. Holliday and J. M. Thornton, *J. Biol. Inorg. Chem.*, 2008, **13**, 1205–1218.
2 D. C. Johnson, D. R. Dean, A. D. Smith and M. K. Johnson, *Annu. Rev. Biochem.*, 2005, **74**, 247–281.
3 M. Richter, *Nat. Prod. Rep.*, 2013, **30**, 1324–1345.
4 J. D. Fischer, G. L. Holliday, S. A. Rahman and J. M. Thornton, *J. Mol. Biol.*, 2010, **403**, 803–824.
5 J. G. Hauge, *J. Biol. Chem.*, 1964, **239**, 3630–3639.
6 J. A. Duine, *J. Biosci. Bioeng.*, 1999, **88**, 231–236.
7 S. A. Salisbury, H. S. Forrest, W. B. Cruse and O. Kennard, *Nature*, 1979, **280**, 843–844.
8 C. Anthony and L. J. Zatman, *Biochem. J.*, 1967, **104**, 960–969.
9 Y. He, Z. Xie, H. Zhang, W. Liebl, H. Toyama and F. Chen, *Front. Microbiol.*, 2022, **13**, 879246.
10 M. Matsutani and T. Yakushi, *Appl. Microbiol. Biotechnol.*, 2018, **102**, 9531–9540.
11 J. P. Klinman and F. Bonnot, *Chem. Rev.*, 2014, **114**, 4343–4365.
12 Y. Q. Shen, F. Bonnot, E. M. Imsand, J. M. RoseFigura, K. Sjolander and J. P. Klinman, *Biochemistry*, 2012, **51**, 2265–2275.
13 C. Anthony, *Antioxid. Redox Signaling*, 2001, **3**, 757–774.
14 P. M. Goodwin and C. Anthony, *Adv. Microb. Physiol.*, 1998, **40**, 1–80.
15 P. G. Arnison, M. J. Bibb, G. Bierbaum, A. A. Bowers, T. S. Bugni, G. Bulaj, J. A. Camarero, D. J. Campopiano, G. L. Challis, J. Clardy, P. D. Cotter, D. J. Craik, M. Dawson, E. Dittmann, S. Donadio, P. C. Dorrestein, K. D. Entian, M. A. Fischbach, J. S. Garavelli, U. Goransson, C. W. Gruber, D. H. Haft, T. K. Hemscheidt, C. Hertweck, C. Hill, A. R. Horswill, M. Jaspars, W. L. Kelly, J. P. Klinman, O. P. Kuipers, A. J. Link, W. Liu, M. A. Marahiel, D. A. Mitchell, G. N. Moll, B. S. Moore, R. Muller, S. K. Nair, I. F. Nes, G. E. Norris, B. M. Olivera, H. Onaka, M. L. Patchett, J. Piel, M. J. Reaney, S. Rebuffat, R. P. Ross, H. G. Sahl, E. W. Schmidt, M. E. Selsted, K. Severinov, B. Shen, K. Sivonen, L. Smith, T. Stein, R. D. Sussmuth, J. R. Tagg, G. L. Tang, A. W. Truman, J. C. Vederas, C. T. Walsh, J. D. Walton, S. C. Wenzel, J. M. Willey and W. A. van der Donk, *Nat. Prod. Rep.*, 2013, **30**, 108–160.
16 W. Zhu and J. P. Klinman, *Curr. Opin. Chem. Biol.*, 2020, **59**, 93–103.
17 M. Mirdita, K. Schutze, Y. Moriwaki, L. Heo, S. Ovchinnikov and M. Steinegger, *Nat. Methods*, 2022, **19**, 679–682.
18 W. Zhu, L. M. Walker, L. Tao, A. T. Iavarone, X. Wei, R. D. Britt, S. J. Elliott and J. P. Klinman, *J. Am. Chem. Soc.*, 2020, **142**, 12620–12634.
19 S. R. Wecksler, S. Stoll, H. Tran, O. T. Magnusson, S. P. Wu, D. King, R. D. Britt and J. P. Klinman, *Biochemistry*, 2009, **48**, 10151–10161.
20 W. Zhu, A. T. Iavarone and J. P. Klinman, *ACS Cent. Sci.*, 2024, **10**, 251–263.
21 I. Barr, J. A. Latham, A. T. Iavarone, T. Chantarojsiri, J. D. Hwang and J. P. Klinman, *J. Biol. Chem.*, 2016, **291**, 8877–8884.
22 J. A. Latham, A. T. Iavarone, I. Barr, P. V. Juthani and J. P. Klinman, *J. Biol. Chem.*, 2015, **290**, 12908–12918.
23 R. L. Evans III, J. A. Latham, Y. Xia, J. P. Klinman and C. M. Wilmot, *Biochemistry*, 2017, **56**, 2735–2746.
24 A. M. Martins, J. A. Latham, P. J. Martel, I. Barr, A. T. Iavarone and J. P. Klinman, *J. Biol. Chem.*, 2019, **294**, 15025–15036.
25 E. M. Koehn, J. A. Latham, T. Armand, R. L. Evans III, X. Tu, C. M. Wilmot, A. T. Iavarone and J. P. Klinman, *J. Am. Chem. Soc.*, 2019, **141**, 4398–4405.
26 F. Bonnot, A. T. Iavarone and J. P. Klinman, *Biochemistry*, 2013, **52**, 4667–4675.
27 S. M. Janes, D. Mu, D. Wemmer, A. J. Smith, S. Kaur, D. Maltby, A. L. Burlingame and J. P. Klinman, *Science*, 1990, **248**, 981–987.
28 W. S. McIntire, D. E. Wemmer, A. Chistoserdov and M. E. Lidstrom, *Science*, 1991, **252**, 817–824.
29 S. X. Wang, M. Mure, K. F. Medzihradszky, A. L. Burlingame, D. E. Brown, D. M. Dooley, A. J. Smith, H. M. Kagan and J. P. Klinman, *Science*, 1996, **273**, 1078–1084.
30 S. Datta, Y. Mori, K. Takagi, K. Kawaguchi, Z. W. Chen, T. Okajima, S. Kuroda, T. Ikeda, K. Kano, K. Tanizawa and F. S. Mathews, *Proc. Natl. Acad. Sci. U. S. A.*, 2001, **98**, 14268–14273.
31 D. H. Haft, *BMC Genomics*, 2011, **12**, 21.
32 J. D. Selengut and D. H. Haft, *J. Bacteriol.*, 2010, **192**, 5788–5798.
33 J. D. Selengut, D. H. Haft, T. Davidsen, A. Ganapathy, M. Gwinn-Giglio, W. C. Nelson, A. R. Richter and O. White, *Nucleic Acids Res.*, 2007, **35**, D260–D264.
34 W. Li, K. R. O'Neill, D. H. Haft, M. DiCuccio, V. Chetvernin, A. Badretdin, G. Coulouris, F. Chitsaz, M. K. Derbyshire, A. S. Durkin, N. R. Gonzales, M. Gwadz, C. J. Lanczycki, J. S. Song, N. Thanki, J. Wang, R. A. Yamashita, M. Yang, C. Zheng, A. Marchler-Bauer and F. Thibaud-Nissen, *Nucleic Acids Res.*, 2021, **49**, D1020–D1028.
35 T. Paysan-Lafosse, M. Blum, S. Chuguransky, T. Grego, B. L. Pinto, G. A. Salazar, M. L. Bileschi, P. Bork, A. Bridge, L. Colwell, J. Gough, D. H. Haft, I. Letunic, A. Marchler-Bauer, H. Mi, D. A. Natale, C. A. Orengo, A. P. Pandurangan, C. Rivoire, C. J. A. Sigrist, I. Sillitoe, N. Thanki, P. D. Thomas, S. C. E. Tosatto, C. H. Wu and A. Bateman, *Nucleic Acids Res.*, 2023, **51**, D418–D427.
36 B. Khaliullin, R. Ayikpoe, M. Tuttle and J. A. Latham, *J. Biol. Chem.*, 2017, **292**, 13022–13033.
37 R. S. Ayikpoe and J. A. Latham, *J. Am. Chem. Soc.*, 2019, **141**, 13582–13591.
38 R. Ayikpoe, J. Salazar, B. Majestic and J. A. Latham, *Biochemistry*, 2018, **57**, 5379–5383.
39 A. A. Dubey and V. Jain, *Appl. Environ. Microbiol.*, 2019, **85**, e00535.
40 R. Plocinska, K. Strus, M. Korycka-Machala, P. Plocinski, M. Kuziola, A. Zaczek, M. Slomka and J. Dziadek, *Front. Cell. Infect. Microbiol.*, 2024, **14**, 1427829.
41 A. P. Graça, V. Nikitushkin, M. Ellerhorst, C. Vilhena, T. E. Klassert, A. Starick, M. Siemers, W. K. Al-Jammal,

I. Vilotijevic, H. Slevogt, K. Papenfort and G. Lackner, *eLife*, 2025, **13**, RP97559.
42 D. H. Haft, P. G. Pierce, S. J. Mayclin, A. Sullivan, A. S. Gardberg, J. Abendroth, D. W. Begley, I. Q. Phan, B. L. Staker, P. J. Myler, V. M. Marathias, D. D. Lorimer and T. E. Edwards, *Sci. Rep.*, 2017, **7**, 41074.
43 M. J. van der Werf, C. van der Ven, F. Barbirato, M. H. Eppink, J. A. de Bont and W. J. van Berkel, *J. Biol. Chem.*, 1999, **274**, 26296–26304.
44 I. Nagy, S. Verheijen, A. De Schrijver, J. Van Damme, P. Proost, G. Schoofs, J. Vanderleyden and R. De Mot, *Arch. Microbiol.*, 1995, **163**, 439–446.
45 A. Norin, S. R. Piersma, J. A. Duine and H. Jornvall, *Cell. Mol. Life Sci.*, 2003, **60**, 999–1006.
46 P. W. Van Ophem, J. Van Beeumen and J. A. Duine, *Eur. J. Biochem.*, 1993, **212**, 819–826.
47 P. Schenkels and J. A. Duine, *Microbiology*, 2000, **146**(Pt 4), 775–785.
48 L. V. Bystrykh, N. I. Govorukhina, P. W. Van Ophem, H. J. Hektor, L. Dijkhuizen and J. A. Duine, *J. Gen. Microbiol.*, 1993, **139**, 1979–1985.
49 L. V. Bystrykh, J. Vonck, E. F. J. Van Bruggen, J. Van Beeumen, B. Samyn, N. I. Govorukhina, N. Arfman, J. A. Duine and L. Dijkhuizen, *J. Bacteriol.*, 1993, **175**, 1814–1822.
50 H. Park, H. Lee, Y. T. Ro and Y. M. Kim, *Microbiology*, 2010, **156**, 463–471.
51 A. A. Dubey, S. R. Wani and V. Jain, *J. Bacteriol.*, 2018, **200**, DOI: **10.1128/jb.00288-18**.
52 N. Ohhata, N. Yoshida, H. Egami, T. Katsuragi, Y. Tani and H. Takagi, *J. Bacteriol.*, 2007, **189**, 6824–6831.
53 L. Peña-Ortiz, A. P. Graça, H. J. Guo, D. Braga, T. G. Köllner, L. Regestein, C. Beemelmanns and G. Lackner, *Chem. Sci.*, 2020, **11**, 5182–5190.
54 M. Ellerhorst, S. A. Barth, A. P. Graça, W. K. Al-Jammal, L. Peña-Ortiz, I. Vilotijevic and G. Lackner, *ACS Chem. Biol.*, 2022, **17**, 3207–3217.
55 M. L. Ellinwood, Master's thesis, University of Denver, 2020.
56 C. L. M. Gilchrist and Y. H. Chooi, *Bioinformatics*, 2021, **37**, 2473–2475.
57 R. Ayikpoe, V. Govindarajan and J. A. Latham, *Appl. Microbiol. Biotechnol.*, 2019, **103**, 2903–2912.
58 N. A. Bruender and V. Bandarian, *J. Biol. Chem.*, 2017, **292**, 4371–4381.
59 T. Shimizu, K. Suzuki and M. Inui, *Appl. Microbiol. Biotechnol.*, 2024, **108**, 58.
60 N. Van Wyk, D. Navarro, M. Blaise, J. G. Berrin, B. Henrissat, M. Drancourt and L. Kremer, *Glycobiology*, 2017, **27**, 392–399.
61 O. Dym and D. Eisenberg, *Protein Sci.*, 2001, **10**, 1712–1728.
62 H. Qi, I. Atkinson, S. Xiao, Y. J. Choi, T. Tobimatsu and B. Shane, *Adv. Enzyme Regul.*, 1999, **39**, 263–273.
63 B. Ney, C. R. Carere, R. Sparling, T. Jirapanjawat, M. B. Stott, C. J. Jackson, J. G. Oakeshott, A. C. Warden and C. Greening, *Front. Microbiol.*, 2017, **8**, 1902.
64 C. Greening, F. H. Ahmed, A. E. Mohamed, B. M. Lee, G. Pandey, A. C. Warden, C. Scott, J. G. Oakeshott, M. C. Taylor and C. J. Jackson, *Microbiol. Mol. Biol. Rev.*, 2016, **80**, 451–493.
65 C. A. Abbas and A. A. Sibirny, *Microbiol. Mol. Biol. Rev.*, 2011, **75**, 321–360.
66 D. Last, M. Hasan, L. Rothenburger, D. Braga and G. Lackner, *Metab. Eng.*, 2022, **73**, 158–167.
67 J. B. Taylor, *Trans. Faraday Soc.*, 1957, **53**, 1198–1203.
68 J. E. Griffin, J. D. Gawronski, M. A. Dejesus, T. R. Ioerger, B. J. Akerley and C. M. Sassetti, *PLoS Pathog.*, 2011, **7**, e1002251.
69 G. Krishnamoorthy, P. Kaiser, L. Lozza, K. Hahnke, H. J. Mollenkopf and S. H. E. Kaufmann, *mBio*, 2019, **10**, e00190–e00119.
70 S. R. Wani and V. Jain, *Protein Sci.*, 2022, **31**, 628–638.
71 L. Peña-Ortiz, I. Schlembach, G. Lackner and L. Regestein, *Front. Bioeng. Biotechnol.*, 2020, **8**, 593781.
72 R. Roccor, M. E. Wolf, J. Liu and L. D. Eltis, *Appl. Environ. Microbiol.*, 2024, **90**, e0041624.
73 D. Vargas, S. Hageman, M. Gulati, C. J. Nobile and M. Rawat, *IUBMB Life*, 2016, **68**, 621–628.
74 K. S. Wong and W. A. Houry, *J. Struct. Biol.*, 2012, **179**, 211–221.
75 M. Kahle, S. Appelgren, A. Elofsson, M. Carroni and P. Ädelroth, *BMC Biol.*, 2023, **21**, 47.
76 G. Krishnamoorthy, P. Kaiser, P. Constant, U. Abu Abed, M. Schmid, C. K. Frese, V. Brinkmann, M. Daffe and S. H. E. Kaufmann, *mBio*, 2021, **12**, e0166521.
77 V. Nikitushkin, M. Shleeva, D. Loginov, F. F. Dycka, J. Sterba and A. Kaprelyants, *PLoS One*, 2022, **17**, e0269847.
78 A. Mendauletova and J. A. Latham, *J. Biol. Chem.*, 2022, **298**, 101474.
79 F. Peng, Z. H. Ke, H. R. Jin, W. Wang, H. R. Zhang and Y. Li, *FASEB J.*, 2024, **38**, e23724.
80 M. Blum, A. Andreeva, L. C. Florentino, S. R. Chuguransky, T. Grego, E. Hobbs, B. L. Pinto, A. Orr, T. Paysan-Lafosse, I. Ponamareva, G. A. Salazar, N. Bordin, P. Bork, A. Bridge, L. Colwell, J. Gough, D. H. Haft, I. Letunic, F. Llinares-Lopez, A. Marchler-Bauer, L. Meng-Papaxanthos, H. Mi, D. A. Natale, C. A. Orengo, A. P. Pandurangan, D. Piovesan, C. Rivoire, C. J. A. Sigrist, N. Thanki, F. Thibaud-Nissen, P. D. Thomas, S. C. E. Tosatto, C. H. Wu and A. Bateman, *Nucleic Acids Res.*, 2025, **53**, D444–D456.
81 J. Abramson, J. Adler, J. Dunger, R. Evans, T. Green, A. Pritzel, O. Ronneberger, L. Willmore, A. J. Ballard, J. Bambrick, S. W. Bodenstein, D. A. Evans, C. C. Hung, M. O'Neill, D. Reiman, K. Tunyasuvunakool, Z. Wu, A. Zemgulyte, E. Arvaniti, C. Beattie, O. Bertolli, A. Bridgland, A. Cherepanov, M. Congreve, A. I. Cowen-Rivers, A. Cowie, M. Figurnov, F. B. Fuchs, H. Gladman, R. Jain, Y. A. Khan, C. M. R. Low, K. Perlin, A. Potapenko, P. Savy, S. Singh, A. Stecula, A. Thillaisundaram, C. Tong, S. Yakneen, E. D. Zhong, M. Zielinski, A. Zidek, V. Bapst, P. Kohli, M. Jaderberg, D. Hassabis and J. M. Jumper, *Nature*, 2024, **630**, 493–500.
82 M. J. van der Werf and A. M. Boot, *Microbiology*, 2000, **146**(Pt 5), 1129–1141.

83 A. Singh, S. Jain, S. Gupta, T. Das and A. K. Tyagi, *FEMS Microbiol. Lett.*, 2003, **227**, 53–63.
84 H. J. Hektor and L. Dijkhuizen, *FEMS Microbiol. Lett.*, 1996, **144**, 73–79.
85 I. Nagy, G. Schoofs, F. Compernolle, P. Proost, J. Vanderleyden and R. De Mot, *J. Bacteriol.*, 1995, **177**, 676–687.
86 I. Nagy, F. Compernolle, K. Ghys, J. Vanderleyden and R. De Mot, *Appl. Environ. Microbiol.*, 1995, **61**, 2056–2060.
87 A. A. Dubey and V. Jain, *Biochem. Biophys. Res. Commun.*, 2019, **516**, 1073–1077.
88 D. R. Cavener, *J. Mol. Biol.*, 1992, **223**, 811–814.
89 M. Berney and G. M. Cook, *PLoS One*, 2010, **5**, e8614.
90 O. Trott and A. J. Olson, *J. Comput. Chem.*, 2010, **31**, 455–461.
91 N. F. S. K. Anuar, F. Huyop, G. Ur-Rehman, F. Abdullah, Y. M. Normi, M. K. Sabullah and R. A. Wahab, *Int. J. Mol. Sci.*, 2022, **23**, 12644.
92 K. A. Abrahams, S. M. Batt, S. S. Gurcha, N. Veerapen, G. Bashiri and G. S. Besra, *Nat. Commun.*, 2023, **14**, 3828.